SEMMELWEIS EGYETEM

DOKTORI ISKOLA

Ph.D. értekezések

3541.

BORBOLA DÁNIEL JÓZSEF

Fogorvostudományi kutatások

című program

Programvezető: Dr. Varga Gábor, egyetemi tanár

Témavezető: Dr. Vág János, egyetemi tanár

Development and Validation of a Novel Virtual-Fit Method for Evaluating Intraoral Scanner Accuracy

Ph.D. Thesis

Dániel József Borbola DMD

Division of Dental Research
Semmelweis University Doctoral School





Supervisor: János Vág, DMD, DSc.
Official reviewers: Dóra Haluszka, PhD.
Márk Tibor Fráter, DMD, DSc.

Head of the Complex Examination Committee:
Gábor Gerber, DMD, PhD, Habil.

Members of the Complex Examination Committee:
Árpád Joób-Fancsaly, DMD, PhD, Habil.
Ákos Nagy, DMD, PhD, Habil.

Budapest
2026

TABLE OF CONTENTS

LIST OF ABBREVATIONS 4

1. INTRODUCTION 5

2. OBJECTIVES 9

2.1 Application of the virtual-fit method for fixed complete denture cases designed on intraoral scans: Effect of cement spacing – Study 1 9

2.2 Complete-arch accuracy of seven intraoral scanners measured by the virtual-fit method – Study 2 10

3. METHODS 11

3.1 Application of the virtual-fit method for fixed complete denture cases designed on intraoral scans: Effect of cement spacing – Study 1 11

3.1.1 Model fabrication and scanning 11

3.1.2 Scan segmentation 11

3.1.3 Framework design 13

3.1.4 Measurements 15

3.1.5 Statistics 17

3.2 Complete-arch accuracy of seven intraoral scanners measured by the virtual-fit method - Study 2 18

3.2.1 Model fabrication and scanning 18

3.2.2 Scan segmentation 21

3.2.3 Framework design 21

3.2.4 Measurements 23

3.2.5 Sample size estimation 23

3.2.6 Statistics 24

4. RESULTS 25

4.1. Application of the virtual-fit method for fixed complete denture cases designed on intraoral scans: Effect of cement spacing – Study 1 25

4.1.1 Validation of gap measurement 25
4.1.2 Validation of the virtual-fit method 26
4.1.3 Accuracy of intraoral scanners 26
4.2 Complete-arch accuracy of seven intraoral scanners measured by the virtual-fit method - Study 2 31
4.2.1 Median marginal gap (trueness) 31
4.2.2 Median internal gap (trueness) 32
4.2.3 Mean absolute error (precision) of the marginal gap 33
4.2.4 Mean absolute error (precision) of the internal gap 35
5. DISCUSSION 37
5.1 Application of the virtual-fit method for fixed complete denture cases designed on intraoral scans: Effect of cement spacing – Study 1 38
5.2 Complete-arch accuracy of seven intraoral scanners measured by the virtual-fit method – Study 2 40
6. CONCLUSIONS 45
6.1 Application of the virtual-fit method for fixed complete denture cases designed on intraoral scans: Effect of cement spacing – Study 1 45
6.2 Complete-arch accuracy of seven intraoral scanners measured by the virtual-fit method – Study 2 46
7. SUMMARY 47
8. REFERENCES 48
9. BIBLIOGRAPHY OF PUBLICATIONS 55
9.1 Publications directly related to the thesis: 55
9.2 Publications indirectly related to the thesis: 56
10. ACKNOWLEDGEMENTS 57

LIST OF ABBREVATIONS

AI - Artificial intelligence

CAD - Computer-aided design

CAM - Computer-aided manufacturing

ICP - Iterative closest point algorithm

IOS - Intraoral scanner

MAD - Mean absolute deviation

MAE - Mean absolute error

MG - Marginal gap

RMS - Root mean square

SD - Standard deviation

STL - Standard Tessellation Language

2D - Two-dimensional

3D - Three-dimensional

1. INTRODUCTION

The long-term success of tooth-supported dental prostheses is principally dependent on the accuracy of fit between the restoration and the prepared abutment teeth, as well as on several other factors, including marginal fit and adaptation (1), abutment tooth preparation, proper material selection (2), and cementation protocol (3). It is widely accepted in dentistry that inadequate marginal and/or internal adaptation of the restoration might lead to biological and structural complications such as secondary caries (4), periodontal inflammation (5), as well as technical failures, including debonding (6) and fracture (7). Evaluation and optimization of restoration fit has remained a central topic in prosthodontic research for decades (8, 9). With the rapid development of digital workflows and intraoral scanning technologies, the traditional paradigms used to assess prosthetic accuracy are being increasingly challenged (10). Improved accuracy in computer-aided design and computer-aided manufacturing (CAD/CAM) workflow contributes to better retention, reduced microleakage, and enhanced long-term clinical performance of restorations (11).

Digital impression technique with the help of intraoral scanners (IOSs) has become an integral part of contemporary prosthodontics, offering advantages such as improved patient comfort, streamlined workflows, and seamless integration with CAD/CAM systems. While their accuracy for single-unit restorations and short-span fixed partial dentures has been well documented (12), the reliability of IOSs for complete-arch fixed prostheses remains controversial, primarily due to the accumulation of stitching errors and angular deviations over long-span scans, which may adversely affect prosthetic fit and clinical performance (13). Complete-arch scans are inherently susceptible to cumulative stitching errors, and even minor deviations may result in clinically relevant misfit when propagated across long spans (14). This issue is particularly critical in tooth-supported fixed complete-arch restorations, where rigid connections between abutments limit the adaptive capacity of the prosthesis, while periodontal ligaments might lead to some compensation effect (15). Furthermore, artifical intelligence (AI) and machine learning algorithms may help predict inaccuracies associated with milling or sintering processes and compensate for them during the digital design workflow phase, thereby increasing the precision and reproducibility of CAD/CAM-made restorations (16).

The majority of available evidence suggests that studies evaluating IOS accuracy have relied on conventional accuracy metrics, typically quantified by the mean absolute distance (MAD) or root mean square (RMS) deviation following scan-to-scan superimposition with a reference model (17, 18). Although these metrics are useful for relative comparison between scanners, they are derived from virtual alignment procedures that permit surface interpenetration during iterative closest point (ICP) alignment (19). Such penetration introduces a non-physical degree of freedom, allowing scans to "sink into" each other and thereby minimizing measured deviations. As a result, conventional trueness metrics may significantly underestimate the actual discrepancy that would occur during physical seating of a restoration (20).

This methodological limitation creates a fundamental disconnect between digital accuracy studies and clinical reality. Clinicians evaluate restoration accuracy in terms of marginal and internal gaps, which are measured after seating a rigid prosthesis onto rigid abutments under standardized conditions in in vitro investigations, where clinical variability such as periodontal ligament resilience and biological response is not present. (13, 14). In contrast, conventional IOS accuracy studies report abstract numerical values in two dimensions (2D) that cannot be directly translated into clinically interpretable parameters (21). This discrepancy has led to uncertainty regarding acceptable IOS accuracy thresholds for complete-arch restorations and has contributed to inconsistent recommendations across the literature (22).

An additional complexity arises from the role of cement spacing in CAD design. Cement space is introduced between the restoration and the abutment to facilitate seating, accommodate manufacturing tolerances, and allow uniform cement distribution (23). However, the optimal cement space for digitally fabricated complete-arch prostheses remains not clearly established in the literature, due to variability in manufacturing workflows, scanner accuracy, and material-dependent fabrication protocols (24). While increasing cement spacing may compensate for scanning or manufacturing inaccuracies, excessive spacing has been associated with increased marginal discrepancies, reduced retention, and unfavorable stress distribution within the cement layer (25). Despite its clinical importance, cement spacing is rarely incorporated into IOS accuracy studies, which typically evaluate scans independently of the restorative design parameters that ultimately determine clinical seating/fit.

Against this background, a critical methodological gap becomes apparent: current IOS accuracy assessment methods do not adequately simulate the clinical process of restoration seating, nor do they account for the compensatory role of cement spacing within a digital workflow. Addressing this gap requires an evaluation framework that integrates scanning accuracy, CAD design parameters, and clinically relevant fit outcomes on a common scale.

The first study presented in this thesis introduces and validates a novel *virtual-fit* method designed to bridge this gap (24, 26). Unlike conventional scan-to-scan superimposition, the virtual-fit approach employs a non-penetrating ICP alignment that prevents virtual interpenetration between the restoration design and the reference model (27). By digitally "seating" a CAD-designed framework onto reference abutments under physical circumstances, this method simulates the clinical try-in of a fixed prosthesis. Importantly, it also allows direct measurement of internal and marginal gap discrepancies. The parameters are comparable to traditional/conventional linear fit assessment techniques such as stereomicroscopy (28), micro-computed tomography (micro-CT) (14), and the silicone replica technique (29, 30). Although these techniques are widely accepted, they are based on two-dimensional (2D) cross-sectional measurements, typically performed at only four discrete locations per crown (mesiodistal and buccolingual directions) (28, 30). As a result, they may question whether they can adequately represent the complete three-dimensional (3D) characteristics of marginal adaptation (31). This limited spatial resolution increases the likelihood of underestimating localized discrepancies and necessitates repeated measurements to achieve representative results (32). The triple-scan protocol enables 3D assessment of the marginal region; however, it is based on a surface comparison method that evaluates an area extending from the restoration margin (33). During the CAD design process, cement space parameters are generally set considerably lower in the marginal region (typically 0–20 μm) compared with the internal area (typically 30–200 μm) (23).

Considering the above explained measurement challenges, the first study systematically investigated the effect of different cement spacing configurations on the internal and marginal fit of complete-arch fixed prostheses designed from intraoral scans. While the first study established the conceptual and methodological validity of the novel virtual-fit

approach, its scope was intentionally limited to a small number of IOS systems to ensure rigorous validation.

The second study extended this framework to a broader comparative analysis of seven IOSs, thereby addressing a clinically relevant question: which scanners are suitable for complete-arch fixed prosthodontics when evaluated using a clinically realistic metric? By applying the virtual-fit method to a diverse pool of scanners with varying technological backgrounds and market positions, the second study provided a comprehensive assessment of both trueness and precision at the level of marginal and internal gaps. Importantly it should be highlighted that IOS accuracy cannot be meaningfully interpreted in isolation from the restorative workflow in which the scan is used and the manufacturing step of CAD/CAM workflow might also lead to increasing misfit of restoration (23, 34).

2. OBJECTIVES

The overall aim of this thesis is to introduce and validate a **c**linically realistic novel evaluation method for measuring intraoral scanner accuracy in tooth-supported complete-arch fixed prosthodontics. The thesis also seeks to bridge the gap between conventional digital accuracy metrics and clinically meaningful fit outcomes by integrating scanning accuracy, CAD design parameters, and restoration seating behavior into a unified evaluation approach.

By addressing these objectives, the thesis aims to improve and validate the novel virtual-fit method and apply it as an established tool/method for intraoral scanner accuracy, translating the values into evidence-based results.

2.1 Application of the virtual-fit method for fixed complete denture cases designed on intraoral scans: Effect of cement spacing – Study 1

1. **To validate the virtual-fit alignment algorithm** by assessing whether the measured internal and marginal gaps correspond to the predefined cement space settings when a CAD-designed complete-arch framework is virtually seated on tooth abutments.

   Null hypothesis #1: The internal and marginal gaps do not significantly deviate from the preset cement space values.
2. **To investigate the effect of cement spacing on the accuracy of intraoral scanner by means of the virtual-fit method** in complete-arch fixed restorations design.

   Null hypothesis #2: Internal and marginal gaps do not differ significantly across different cement spacing settings.
3. **To assess the relationship between the virtual-fit method and conventional trueness measurements.**

   Null hypothesis #3: No significant correlation exists between virtual-fit approach and conventional trueness method.

2.2 Complete-arch accuracy of seven intraoral scanners measured by the virtual-fit method – Study 2

1. **To compare the complete-arch accuracy (trueness and precision) of seven different intraoral scanners** by the virtual-fit method.
   Null hypothesis #4: No differences in accuracy (treueness and precision) between the evaluated seven IOSs.
2. **Comparing the effect of two cement spacings on accuracy** across intraoral scanners.
   Null hypothesis #5: Internal and marginal gaps do not differ significantly across the two cement space settings.

3. METHODS

3.1 Application of the virtual-fit method for fixed complete denture cases designed on intraoral scans: Effect of cement spacing – Study 1 *(in vitro)*

3.1.1 Model fabrication and scanning

Four different maxillary arches with tooth abutments were 3D-printed by an Asiga Pro 4K80 UV 3D printer (Asiga Co., Australia) with a resolution of 50 μm in the Z and 56 μm in the X-Y axes. Each model was prepared for a fixed complete prosthesis (Figure 1). The number of abutments (eight, nine, twelve, and seven, respectively) and their locations were different in the four models (A, B, C, D). Each of the dental models was scanned by an industrial scanner with a 12-megapixel camera (ATOS Capsule MV120, Carl Zeiss GOM Metrology GmbH, Germany, software version Hotfix 5.0), with a precision of 1.7 μm. The four scans served as reference models, i.e., as virtual patients. Each model was also scanned by Emerald S (Planmeca, Finland, software version 6.0.1.812) and Medit i700 (Medit, South Korea, software version 1.8.0) IOSs. Each model was scanned three times by a single operator. The operator had no experience with the two IOSs to exclude bias between the scanners. He received trial training for both systems. The scans were coded according to the model (Figure 1, A-D) and the number of replicates (1-3).

3.1.2 Scan segmentation

The reference and IOS scans were imported in STL file format into the dental lab CAD/CAM software Exocad (Exocad DentalDB, software version 3.0 Galway, Exocad GmbH, Germany). In Exocad, the tooth abutments were digitally segmented from the model by selecting the preparation of the margin. These steps represent the standard technical workflow (Figure 2).

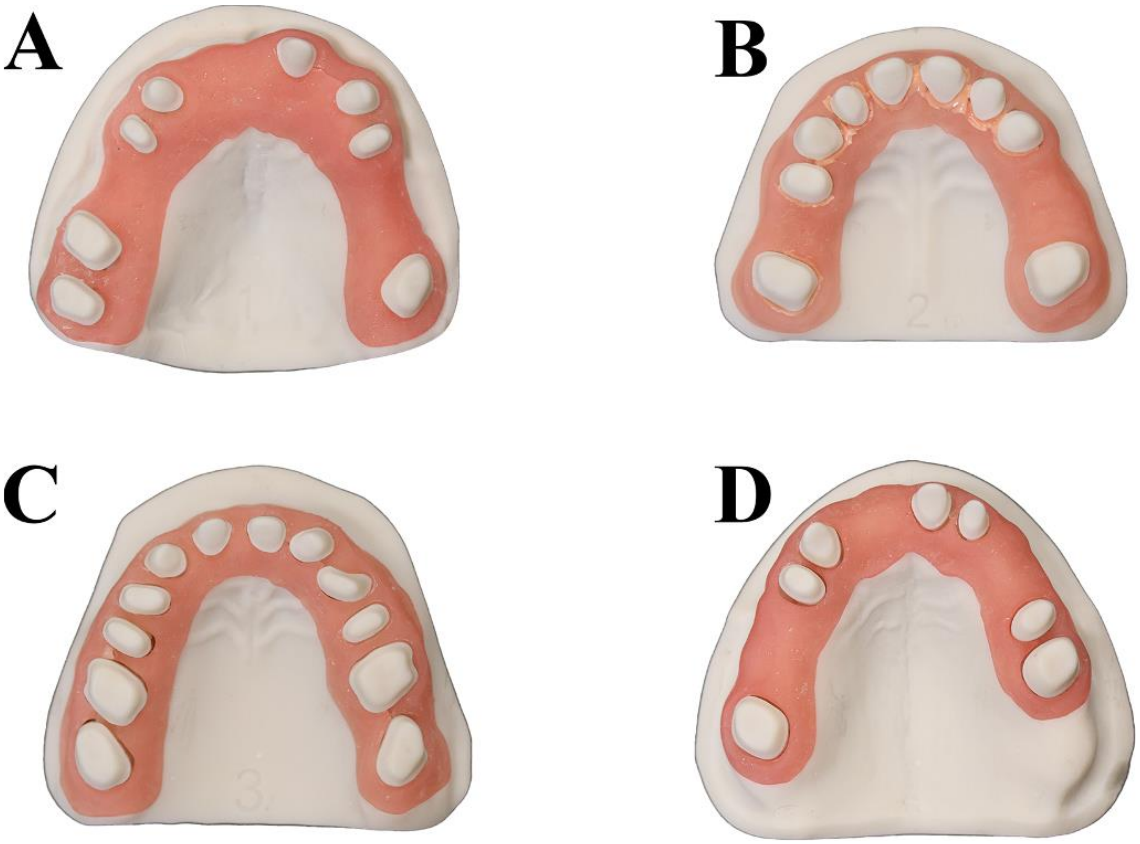


Figure 1. Color photos of the 3D-printed models with teeth abutments and gingiva mask. Model (A) included eight, Model (B) nine, Model (C) twelve, and Model (D) seven abutments. All models represent clinical cases prepared for a fixed complete denture (26).

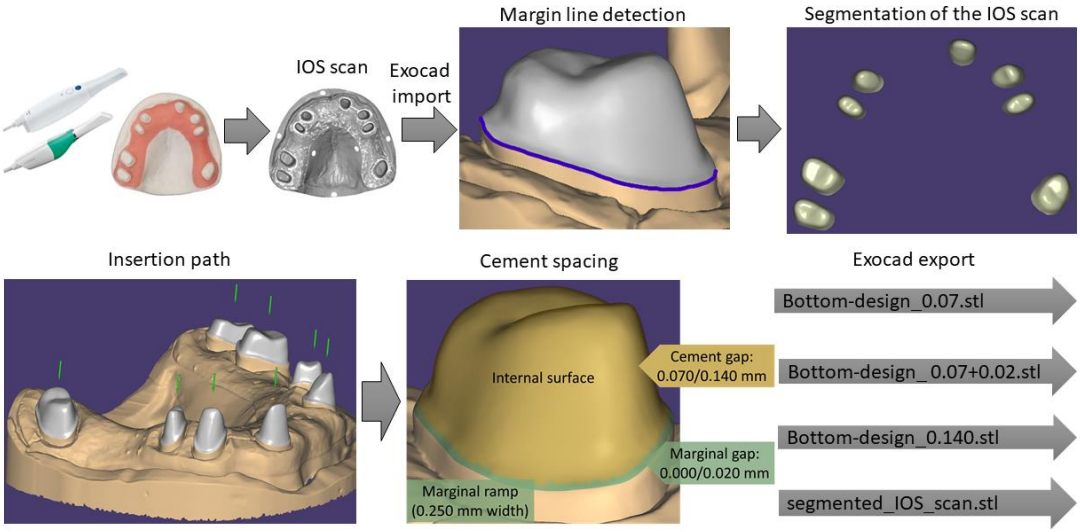


Figure 2. Steps of the Exocad workflow. The workflow shows each step from scanning the models through the design of the virtually designed prostheses in Exocad software to exporting each design with different cement space settings in STL format (26).

3.1.3 Framework design

Three complete-arch tooth-supported fixed prosthesis frameworks with different settings on each IOS scan (two IOSs, four models, three repeats, three cement gaps, $n = 72$) were designed in Exocad. A shared insertion axis was established for all abutments, where crowns are interconnected virtually despite their appearance in the exported design file. The marginal ramp was set to 250 μm for all designs. This function is labeled 'select zones by distance from the margin' (Figure 3). The 'cement gap' setting creates space between the restoration's internal and marginal abutment surface. 'Additional spacing' function adds space between the restoration and the whole abutment surface, including the marginal ramp. According to the settings, three spacing groups were compared (Figure 3).

- Group 70: The 'cement gap' was set at 70 μm without additional spacing.
- Group 70+20: The 'cement gap' was set at 70 μm with 20 μm additional spacing. Therefore, the gap was 20 μm at the marginal ramp and 90 μm at the internal surface area.
- Group 140: The 'cement gap' was set at 140 μm without additional spacing.

The frameworks were exported in STL format and named 'bottom design' (Figure 2). The bottom design contains only the intaglio (internal+marginal) surface of the restoration without the external surface of the full-arch pontics, where cement space parameters are defined to optimize seating and marginal adaptation. This is because the outer layer and the pontics would affect the ICP alignment between the model and the framework.

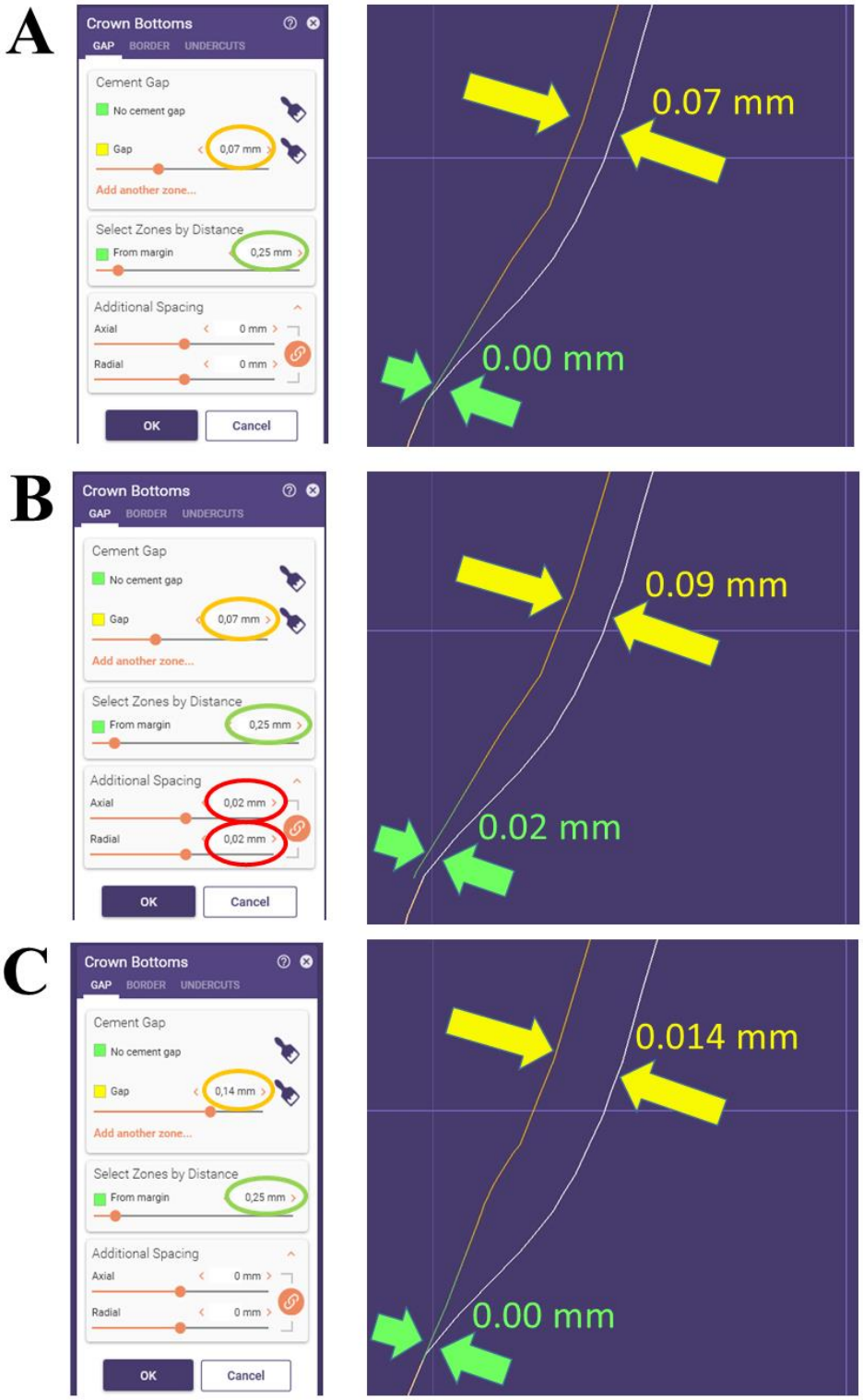


Figure 3. The gap setting panel from the Exocad and the resultant cross-section of tooth 27 in model A in Exocad.

The three different cement spacing groups are indicated: (A) group 70, (B) group 70+20, and (C) group 140 (26).

3.1.4 Measurements

After estabilishing the bottom designs, STL files were imported into Zeiss Inspect 2022 (Carl Zeiss GOM GmbH, Braunschweig, Germany) metrology software for alignments and surface comparisons. Four different types of gap measurements were performed based on mesh type, cement space setting, and comparison area (Figure 4):

• Original (Exocad) position (I.): Bottom designs and corresponding segmented IOS scans were exported from Exocad with identical orientation, preserving the predefined cement spacing. Files were imported into Zeiss Inspect software without further alignment by defining the alignment as the initial alignment. Deviations between the set and measured cemet gaps therefore reflected surface irregularities (Figure 4A).

• Outside-IOS alignment (II.): Following original measurements, bottom designs and IOS scans were aligned using an outside alignment algorithm (ICP-based virtual-fit method preventing mesh penetration). No prealignment was required. Algorithm accuracy was verified by comparing cement gaps obtained before and after outside-IOS alignment (Figure 4A).

• Outside-reference alignment (III.): Bottom designs and segmented reference scans were imported into a separate project, prealigned and subsequently aligned using the same outside alignment algorithm. This approach simulated clinical try-in while excluding fabrication error (Figure 4B).

• Conventional scan-to-scan alignment (IV.): Segmented IOS scans and reference scans (abutments only) were aligned using conventional ICP (prealignment plus best-fit alignment), allowing virtual surface penetration. Three alignments were performed per model and twelve per IOS (Figure 4C).

For all four alignment methods (I-IV.), MAD between the aligned surfaces was calculated in two areas: internal gap area (abutments excluding a 250µm marginal ramp; Figure 5A) and marginal gap area (inverted selection; Figure 5B).

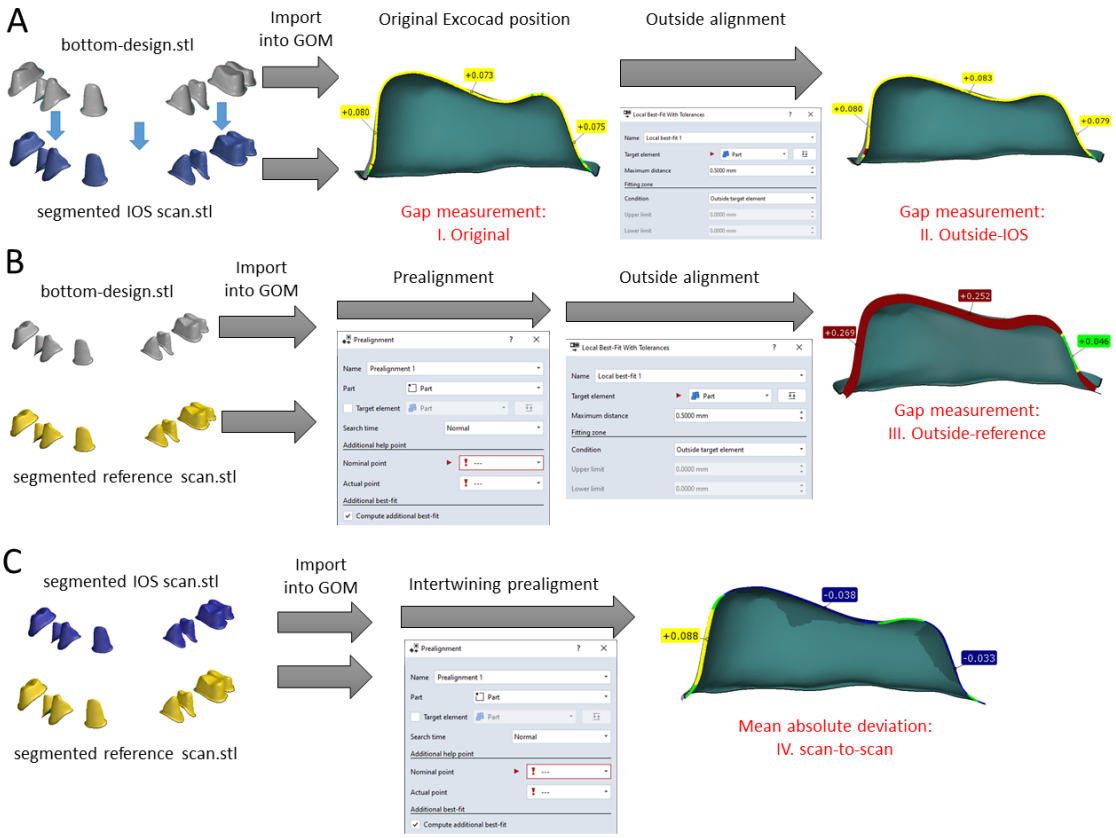


Figure 4. The processing workflow in the Zeiss Inspect software.

The four types of gap measurements based on the alignment are highlighted in red. All images are from a scan of model A made by Medit i700. The cross sections are made at tooth 27 in all images. The bottom design incorporates a cement spacing of 70 µm. The colors between the meshes show the gap size and are categorized as follows: blue for <20 µm, green for 20–70 µm, yellow for 70–90 µm, and red for >90 µm. (A) The bottom design (gray) and the segmented IOS scan (blue) were imported, and their original positions from Exocad were maintained. The gaps were measured without any modifications before aligning the two scans through the outside alignment algorithm using the virtual-fit method. The gaps were then measured again. (B) The bottom design (gray) and the segmented reference scan (yellow) were imported, and a prealignment was conducted. Then, two meshes were aligned by the outside alignment algorithm, after which the resulting gaps were measured. (C) The segmented IOS scan (blue) and the segmented reference scan (yellow) were imported, and prealignment was performed, followed by gap measurement (26).

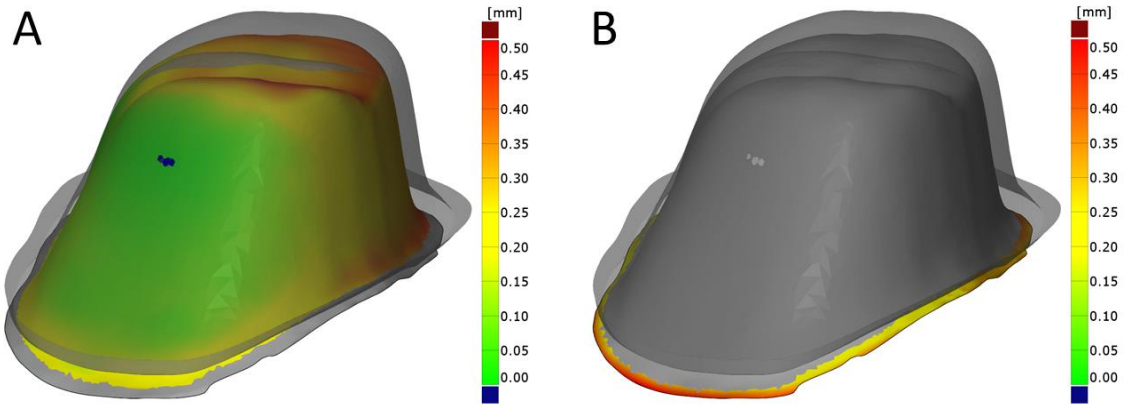


Figure 5. The color-coded surface comparison after outside alignment of the bottom design mesh with IOS scan.

The figure displays a single abutment (tooth 27 in model A) from one of the flawed scans, where the misfit was most pronounced to enhance clarity. (A) The internal surface of all abutments, excluding the 250 µm width margin, was selected for surface comparison. (B) After inverting the selection, the deviation of the marginal area could be measured (26).

3.1.5 Statistics

The descriptive statistics are provided in the dissertation as median, the first (Q1), and the third (Q3) quartiles. The unit of analysis was the 'four models x three repeats', creating an n=12 sample size for each group. The accuracy of the two IOSs was evaluated with the virtual-fit method. The gaps were calculated by removing the outside-IOS gap from the outside-reference gap to eliminate the error in the outside alignment process and unevenness of the Exocad cement spacing. The 100 µm gap was used as a threshold to highlight inferior scans (8).

The MAD of the two IOSs was compared by the Mann–Whitney U Test. The difference between spacing groups was compared by Friedman's Two-Way Analysis of Variance by Ranks. Significance values have been adjusted by the Bonferroni correction for multiple tests.

The correlation between the outside-reference and the scan-to-scan method was evaluated by Spearman's Rho Test. The median of the outside-reference method was compared with that of the scan-to-scan method by the Wilcoxon Signed-Rank Test. The accepted level of statistically significant difference was $p<0.05$. All statistical analyses were done in SPSS (v28, IBM Corp, USA).

3.2 Complete-arch accuracy of seven intraoral scanners measured by the virtual-fit method - Study 2 *(in vitro)*

3.2.1 Model fabrication and scanning

The same 3D-printed resin maxillary arches with various tooth abutments were used to scan and design the full-arch fixed prosthesis. The details of the additive manufacturing of the model were described previously in subsection 3.1.1 (26). Physical dies were made by the same 3D printer (Asiga Pro 4K80 UV, Asiga Co., Australia) utilizing DLP technology with the same settings. Post-processing was done according to the official instructions for use.

The complete workflow, including the scanning and measurements, is shown in Figure 6. Each of the previously created dental models was scanned using an industrial scanner equipped with a 12-megapixel camera (ATOS Q MV100, Carl Zeiss GOM Metrology GmbH, Braunschweig, Germany, software version Zeiss Inspect 2023.2.0.1520), achieving a precision of 1.7 μm on dentate models (26). These four scans were utilized as reference models, functioning as virtual patients.

Each model was scanned by seven intraoral scanners: Aoralscan 3 (Shining3D, Hangzhou, China), Emerald S (Planmeca, Helsinki, Finland), Helios 600 (Eighteeth, Changzhou, China), Lumina (iTero, Align Technology Inc., Tempe, AZ, USA), Medit i700 (Medit, South Korea), Primescan (Dentsply Sirona, Charlotte, NC, USA) and Trios 5 (3Shape A/S, Copenhagen, Denmark). Each model was scanned three times, resulting in 12 scans for each IOS. The optical technology and software versions are listed in Table 1. To ensure independent data acquisition, new scans with newer software versions were performed using the Emerald S and Medit i700 intraoral scanners. Consequently, the scan files from the first study were not included in the present analysis.

All scanning was performed in the same room with the same temperature and lighting conditions. A single operator with general experience in intraoral scanning for more than two years performed all IOS scans to eliminate interoperator bias. The operator received brief training for each IOS system. The scanning strategy for the seven scanners adhered to the manufacturer's recommendations where available.

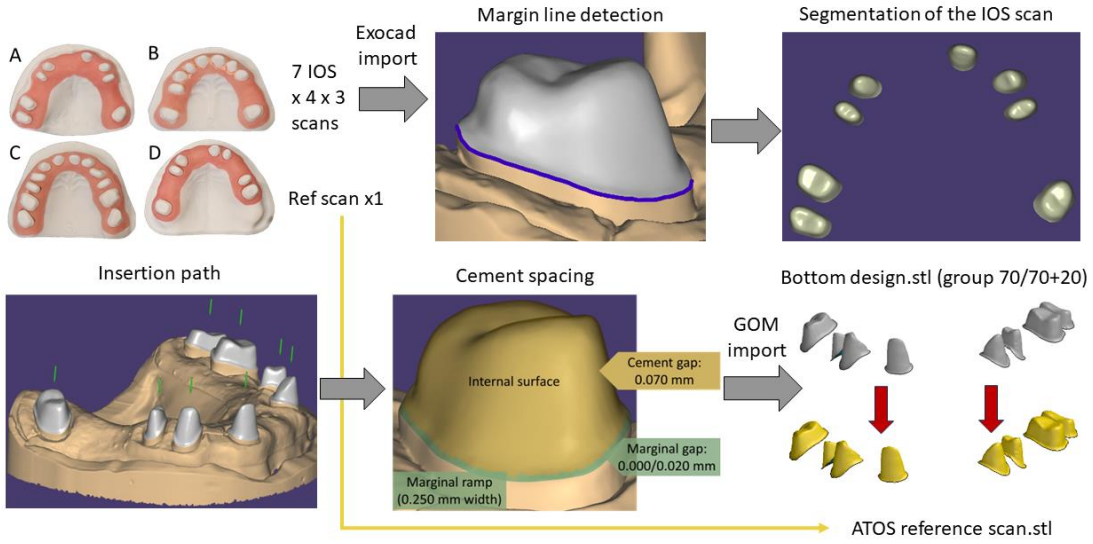


Figure 6. Steps of the Exocad workflow. The IOS (three scans per IOS, each obtained from four models) and reference scans were imported into Exocad software for margin line detection and segmentation, followed by virtual restoration design using two different cement space settings (70 µm and 0 or 20 µm additional spacing) and a 250 µm marginal ramp. The designed restorations were exported as STL files, imported into Zeiss Inspect software, and virtually positioned along the defined insertion path relative to the ATOS Q reference scan for virtual-fit analysis (24).

Table 1. Summary of the features of the evaluated scanners (24).

Name/type of scanner:	Manufacturer of scanner:	Date/year of introduction:	3D optical technology:	Software version*:	Light source:
ATOS Q (100 MV)	Carl Zeiss GOM Metrology GmbH, Braunschweig, Germany	2022 (35)	structured light triangulation	Zeiss Inspect 2023.2.0.1520	blue LED
Emerald S	Planmeca Oy, Helsinki, Finnland	1 October 2019 (36)	structured light triangulation	Romexis 6.4.5.202	blue laser
Medit i700	Medit, Seoul, South Korea	April 2021 (37)	structured light triangulation	Medit link 3.1.4	blue/white LED
Aoralscan 3	Shining 3D, Hangzhou, China	September 2021 (38)	structured light triangulation	IntraoralScan 1.0.0.3305	blue LED
iTero Lumina	Align Technology Inc., Tempe, AZ, USA	February 2024 (39)	Multi-Direct Capture technology™ (triangulation)	3.1.10.607	LED 400-780nm
Helios 600	Eighteeth, Changzhou, China	February 2022 (40)	structured light triangulation	1.1.4.4	blue LED
Primescan	Dentsply Sirona, Charlotte, NC, USA	September 2022 (41)	confocal	Cerec 5.2.4	blue LED
Trios 5	3Shape A/S, Copenhagen, Denmark	2023 (42)	confocal	3Shape Unite 22.1.10.1	LED

***** The listed software versions represented the latest available versions at the time of the study.

3.2.2 Scan segmentation

The reference and IOS scans were imported into Exocad dental lab software (Exocad DentalDB, software version 3.0 Galway, Exocad GmbH, Germany) in STL file format. Within Exocad, the tooth abutments were digitally segmented from the model by delineating the preparation margin (Figure 6), representing the restoration's finish line.

3.2.3 Framework design

Two complete-arch tooth-supported fixed prosthesis frameworks with different cement spacings on each IOS scan (seven IOSs, four models, three repeats, two cement gaps, n=168) were designed in Exocad by a dental technician. The common insertion axis, the pontics connector and the CAD framework design method was conducted in the same way as in the previous study. Marginal ramp was set to 250 μm for all designs (Figure 7). According to the set cement gap and additional spacing function settings, two spacing groups were compared (Figure 7). Further spacing was not applied as it was ineffective in compensating for the scanning error in the previous investigation (26).

- Group 70: the 'cement gap' was set at 70 μm without additional spacing.
- Group 70+20: the 'cement gap' was set at 70 μm with 20 μm additional spacing. Therefore, the gap was 20 μm at the marginal ramp and 90 μm at the internal surface area (Figure 7).

The exported design includes only the intaglio surface of the crown abutments (i.e., the bottom of the design).

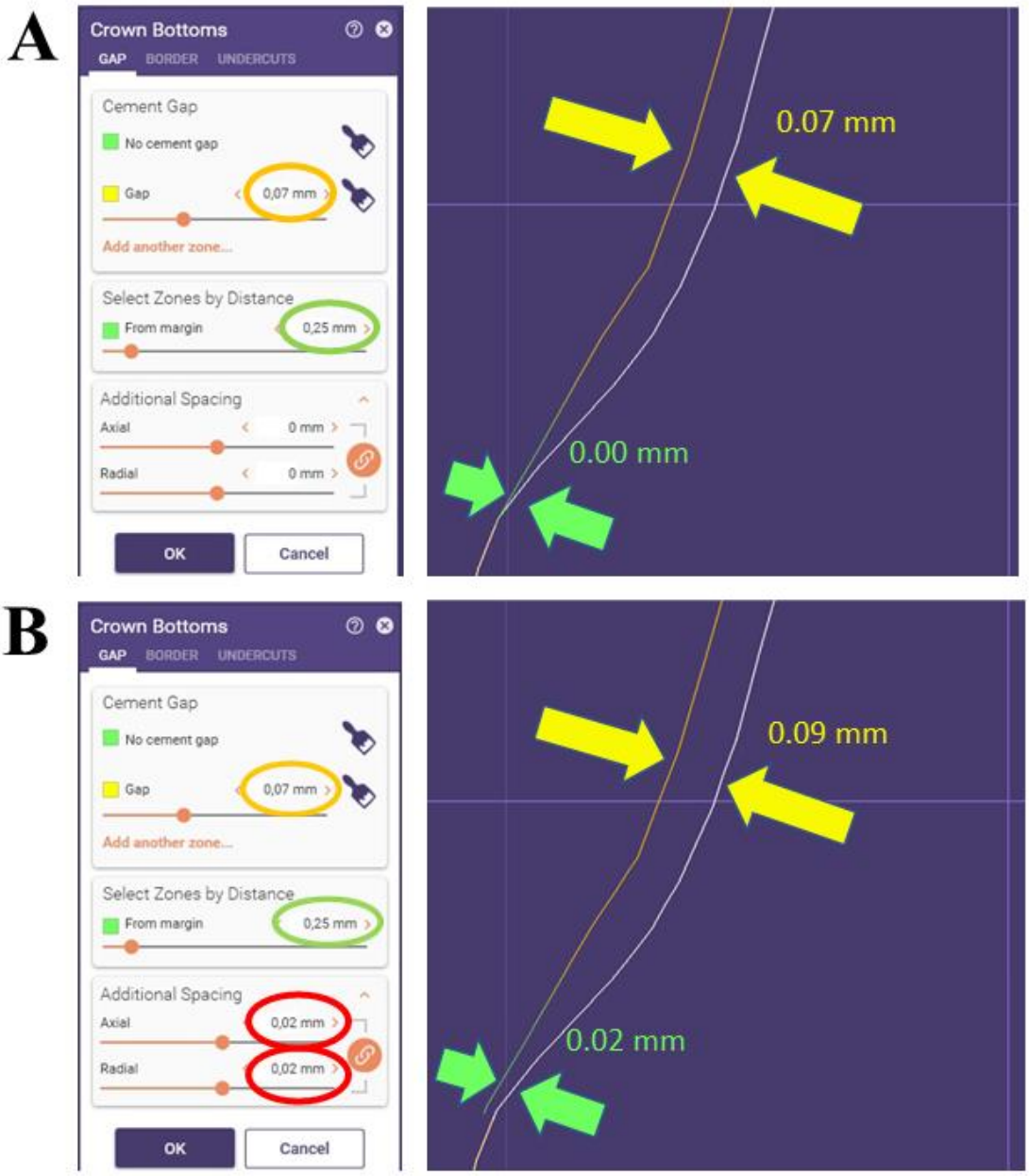


Figure 7. The gap setting panel from Exocad and the resultant cross-section of tooth 27 in model A within Exocad.

Two distinct cement spacing groups were used: (A) group 70 and (B) group 70+20 (24).

3.2.4 Measurements

Each bottom design and the corresponding segmented model made from the reference scan were imported into the same comprehensive metrology program (Zeiss Inspect 2023, Carl Zeiss GmbH, Braunschweig, Germany, version 2023.2.0.1520) (Figure 6). Initially, the bottom design and the reference scan were pre-aligned using the ICP algorithm. Subsequently, the outside alignment algorithm was used. This method virtually fits the design onto the reference model, simulating the actual clinical try-in of the framework. As the framework was not fabricated physically, the virtual-fit method can measure the IOS inaccuracy without fabrication errors.

The mean distance between the aligned surfaces was determined for two specific regions. Initially, the internal cement gap was measured by selecting the abutments without the 250 µm marginal ramp area (Figure 5A). Subsequently, the marginal gap was calculated by selecting a 100 µm area from the finish line (Figure 5B).

3.2.5 Sample size estimation

A priori power analysis was performed using G*Power version 3.1.9.7 (43) to estimate the sample size based on the primary outcome (i.e., the difference in the marginal gap between the seven IOSs) from the previous paper (26). With a significance criterion of $\alpha = 0.05$ and power = 0.80, the minimum sample size required for an effect size of 1.4, according to Cohen (44), was N = 10 for a non-parametric test comparing two independent groups. However, the standard deviation was expected to decrease (and the effect size increased) due to the use of the experienced operator rather than the inexperienced operator in the previous study.

The total number of samples was the combination of replicates x models (the unit of analysis = 12 for each IOS). The "model" is not considered as a fixed factor but as a random factor. Four different models were used to generalize the results for IOS performance.

3.2.6 Statistics

All statistical analyses were performed in SPSS (v28, IBM Corp., USA).

The median gaps of IOSs were compared statistically by the Kruskall- Wallis test due to the violation of the normal distribution assumption of ordinary ANOVA. The groups were categorized into homogeneous subsets. The median gap between cement spacing groups was compared statistically by the Wilcoxon test.

The precision (reproducibility) of the IOSs was estimated by the mean absolute error (MAE) (45). The MAE was calculated by deducing the actual gap values from their respective group means. The MAE of IOSs was compared statistically using the Kruskal-Wallis test. The groups were categorized into homogeneous subsets. The MAE between cement spacing groups was compared statistically by the Wilcoxon test.

4. RESULTS

4.1. Application of the virtual-fit method for fixed complete denture cases designed on intraoral scans: Effect of cement spacing – Study 1 *(in vitro)*

4.1.1 Validation of gap measurement

First, the gap measurement was validated by comparing it to the set cement spacing values in the original position of the bottom design on the model (as they were exported from Exocad). The measured gap was significantly higher in all groups (Table 2) than the set cement space, but the difference ranged only between 0.2–1.7 μm at the internal surface and 3.7–9.9 μm at the margin.

Table 2. The measured gap in micrometers between the bottom design and the IOS scan (26).

		at the internal surface			at the marginal surface		
cement spacing group		set space	original position	outside-alignment (virtual-fit)	set space	original position	outside-alignment (virtual-fit)
70	Median	70 *	71.7 *	73.8 * ##	0	4.0 *	8.8 * ##
	Q1	70	71.70	72.67	0	3.51	8.06
	Q3	70	71.77	75.00	0	4.75	9.91
70+20	Median	70 *	90.2 *	81.4 * ##	20	23.7 *	12.9 * ##
	Q1	70	90.20	80.81	20	23.18	12.70
	Q3	70	90.34	82.06	20	24.22	13.78
140	Median	140 *	141.1 *	141.4 * #	0	9.9 *	12.6 * ##
	Q1	140	141.03	141.25	0	9.28	11.00
	Q3	140	141.29	142.38	0	10.37	14.23

* $p<0.001$ significant deviation from the set space

# $p<0.01$, ## $p<0.001$, original position vs. outside alignment

4.1.2 Validation of the virtual-fit method

Second, the virtual-fit method was validated by comparing the measured gap after the outside alignment of the bottom design with the IOS scan (the scan used for the design) to the measured gap in the original position. The measured gap was significantly higher in groups 70 and 140 (Table 2) than the set cement space and the measured gap in the original position. In group 70+20, both internal and marginal gap was measured significantly less than in the original position due to the additional spacing (20 μm), which allowed the bottom design caps to be seated closer to the abutment.

4.1.3 Accuracy of intraoral scanners

To evaluate the scanning inaccuracy rather than the set cement space, the error at the internal surface was calculated by removing the gap measured with the outside-IOS method (Table 2) from the gap measured with the outside-reference method. The median internal gap error was not different between spacing groups for any IOS (Table 3 and Figure 8). The median internal gap was significantly higher for Medit i700 than for Emerald S in all spacing groups. Additionally, an arbitrary threshold of 100 μm was set to highlight the inferior scans. The internal error was below 100 μm in all cases for Emerald S. However, one scan (A1) of the Medit i700 showed an internal error of 184 μm in group 70 (Figure 9). The error (66 μm) was relieved in group 70+20.

For Emerald S, the median marginal gap in group 140 was significantly higher than in groups 70 and 70+20. For Medit i700, the marginal gap in the 70+20 group was significantly lower than in the 70 and 140 groups (Table 3 and Figure 8). The median marginal gap was significantly higher for Medit i700 than for Emerald S at all cement gap settings. The marginal gap of restorations designed from data using the Emerald S scanner was always below 100 μm (Figure 9). However, it was above 100 μm in 6, 5, and 8 cases in the 70, 70+20, and 140 groups respectively, with Medit i700. Particularly, two scans (A1 and A2) of Medit i700 had extremely high values of 393 μm and 200 μm in group 70. However, these flawed scans produced a reasonably better gap in group 70+20 (A1: 132 μm, A2: 118 μm) and 140 (A1: 112 μm, A2: 124 μm).

The conventional virtual penetrating ICP (scan-to-scan) method provided very similar results in comparison between the two IOSs (Table 3 vs. Table 4). The median error was significantly higher for Medit i700 than for Emerald S at both the internal surface and the

margin (Table 4). However, the conventional method failed to detect outliers (Figure 10). There was a significant correlation between the gaps (virtual-fit method) and the scan-to-scan MAD (conventional trueness) (Table 4 and Figure 11). The measured gap was 2.6–2.8 times higher at the internal gap and 4.0–4.5 times higher at the margin than the scan-to-scan MAD.

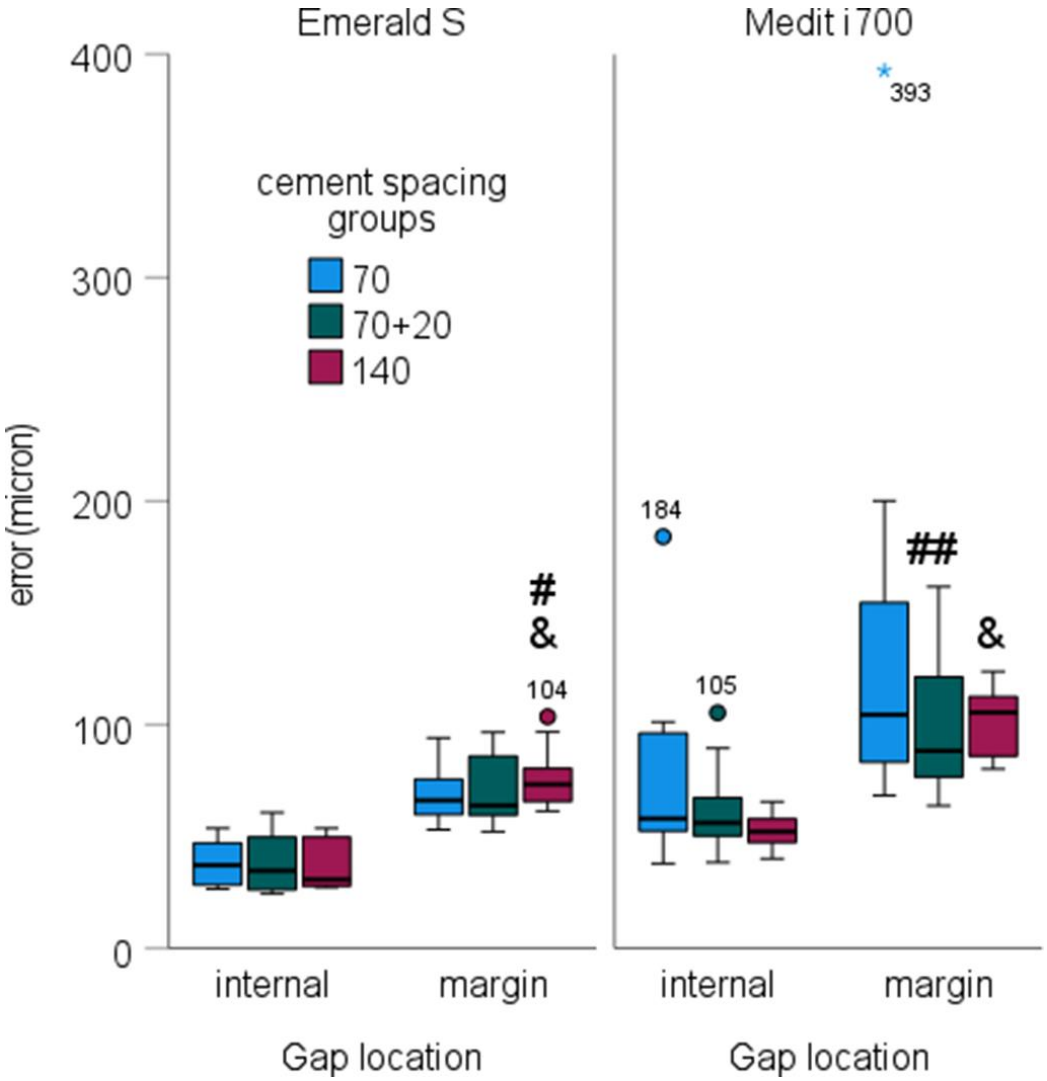


Figure 8. The effect of the cement gap setting on the median error at the internal surface and the margin with two IOSs.

# indicates significant differences compared to the 70 μm setting, # $p<0.05$, ## $p<0.01$, & indicates significant differences between the 140 μm and the 70+20 μm settings, $p<0.05$ (26).

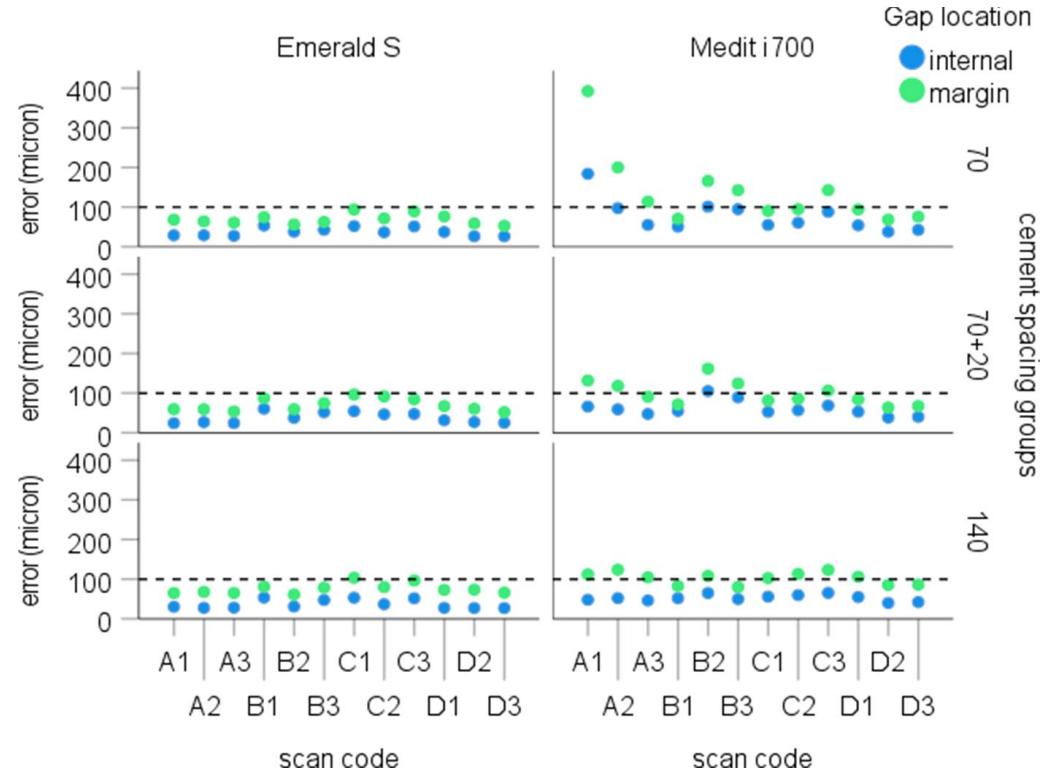


Figure 9. The error at the internal surface and the margin with different cement gap settings and two IOSs. The scans were coded according to the model (A-D, see Figure 1) and the number of replicates (1-3) (26).

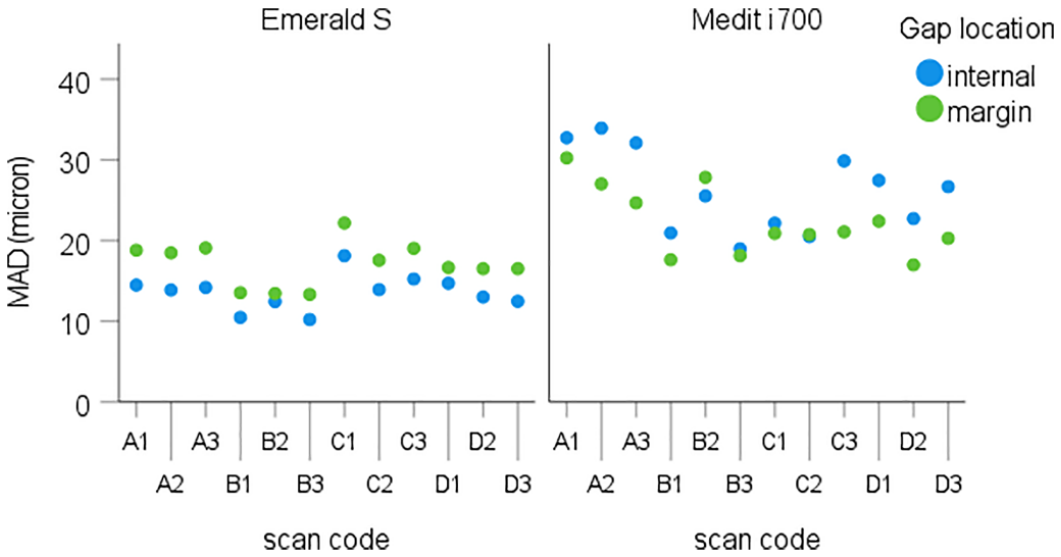


Figure 10. Mean absolute distance (MAD) of the 24 scans, measured at the internal surface and at the margin by the conventional trueness method (scan-to-scan surface comparison) for the two IOSs (Emerald S and Medit i700).

The scans were coded according to the model (A-D, see Figure 1) and the number of replicates (1-3) (26).

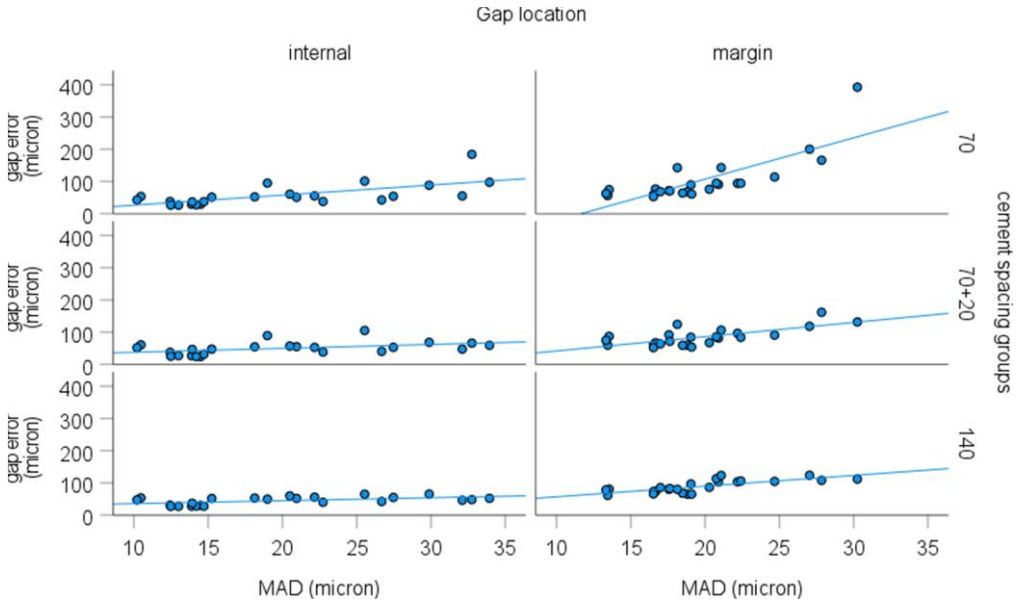


Figure 11. The correlation between the internal error and marginal gap (y-axis) measured by the virtual-fit method (outside-reference) and the mean absolute deviation (MAD, x-axis) measured by the conventional trueness method (scan-to-scan) (26).

Table 3. The scanning error at internal and marginal areas in micrometers (26).

		Gap location			
		internal error°		marginal gap	
cement spacing group		Emerald S	Medit i700	Emerald S	Medit i700
70	Median	**37**	**58** ***	**66**	**104** ***
	Q1	28	53	60	83
	Q2	47	96	76	155
70+20	Median	**35**	**56** **	**64**	**88** * ##
	Q1	26	50	60	77
	Q2	50	67	86	121
140	Median	**31**	**52** **	**73** #, &	**105** *** &
	Q1	28	47	66	86
	Q2	50	58	81	113

° the set cement spacings were deducted from the measured gap to assess the internal errors

* p<0.05, ** p<0.01, *** p<0.001 between scanners

# p<0.05, ## p<0.01 70 µm setting

& p<0.05 140 µm vs. 70+20 µm settings

Table 4. The correlation between the conventional trueness and virtual-fit (26).

cement spacing group	surface	correlation R	fold difference (gap/MAD)
70	internal	0.69 **	2.8 ###
	margin	0.81 **	4.0 ###
70+20	internal	0.51 *	2.7 ###
	margin	0.59 *	4.4 ###
140	internal	0.52 **	2.6 ###
	margin	0.77 **	4.5 ###

* $p<0.05$, ** $p<0.01$.

$p<0.001$ in median

4.2 Complete-arch accuracy of seven intraoral scanners measured by the virtual-fit method - Study 2 *(in vitro)*

4.2.1 Median marginal gap (trueness)

The median marginal gap significantly differed between IOSs in both cement spacing groups. In group 70, the Medit i700, Primescan, and Emerald S were in the best homogenous subset, followed by Lumina, Aoralscan 3, and Trios 5. The median gap in Helios 600 was significantly higher than in all other IOSs. The additional cement spacing (comparing group 70 with group 70+20) significantly decreased the median gap for Lumina and Aoralscan 3. Therefore, in group 70+20, the ranking was only slightly changed. Lumina and Aorlascan 3 were no longer significantly different from Primescan and Emerald S in group 70+20 (Figure 12, Table 5).

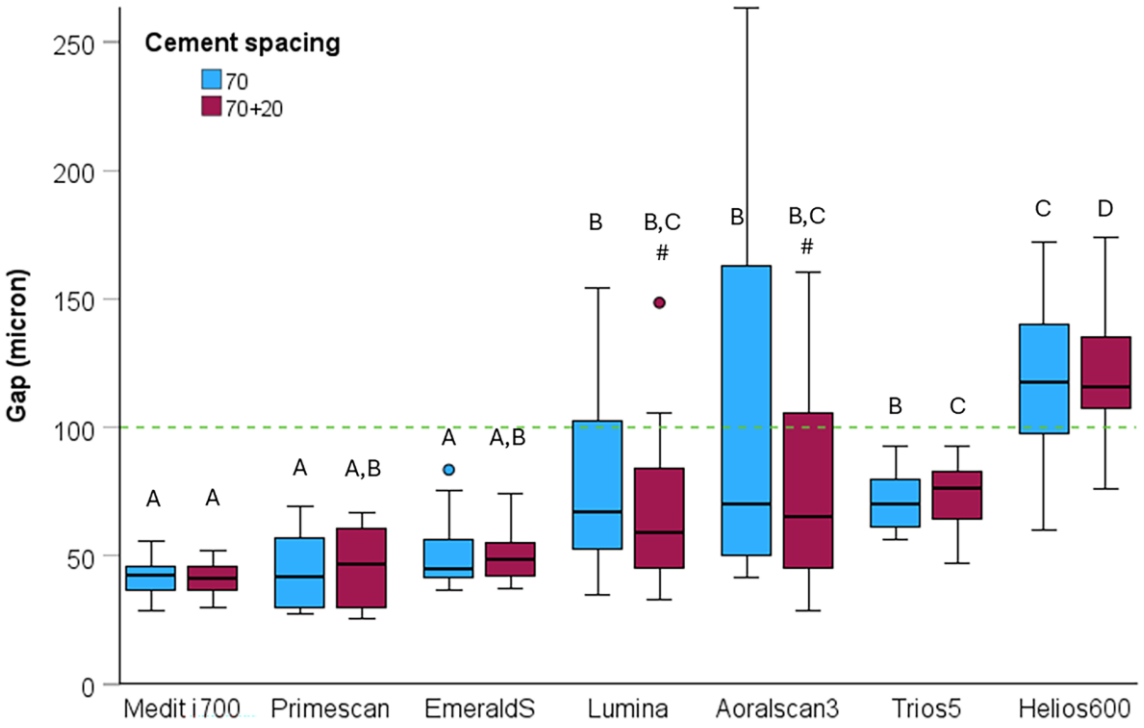


Figure 12. Comparison of the marginal gap between IOSs and cement spacing groups. Different capital letters indicate a significant difference between IOSs within a cement spacing group at $p<0.05$, and # $p<0.05$ between cement spacing groups. The green dotted line depicts the 100 µm clinically acceptable limit (24).

Table 5. Marginal gaps (24).

	Cement spacing									
	70					70+20				
	N	Mean	Median	Q1	Q3	N	Mean	Median	Q1	Q3
Medit i700	12	42	43	37	46	12	41	41	37	46
Primescan	12	44	42	30	57	12	46	47	30	61
Emerald S	12	51	45	41	57	12	50	48	42	55
Lumina	12	80	67	53	103	12	69	59	45	84
Aoralscan 3	12	108	70	50	163	12	78	65	45	105
Trios 5	12	71	70	61	79	12	74	77	64	83
Helios 600	12	118	118	97	140	12	121	116	108	135

4.2.2 Median internal gap (trueness)

The median internal gap was significantly different between IOSs in both cement spacing groups. In group 70, the Medit i700, Primescan, and Emerald S were in the lowest homogenous subset, followed by Aoralscan 3. Trios 5 and Lumina comprised the third subsets. The median internal gap in Helios 600 was significantly higher than all other IOSs. The additional cement spacing (comparing group 70 with group 70+20) slightly but significantly increased the median gap for all IOS except for Lumina. Therefore, the third subset collapsed with the second subset in group 70+20 but kept the same order as in group 70 (Figure 13, Table 6).

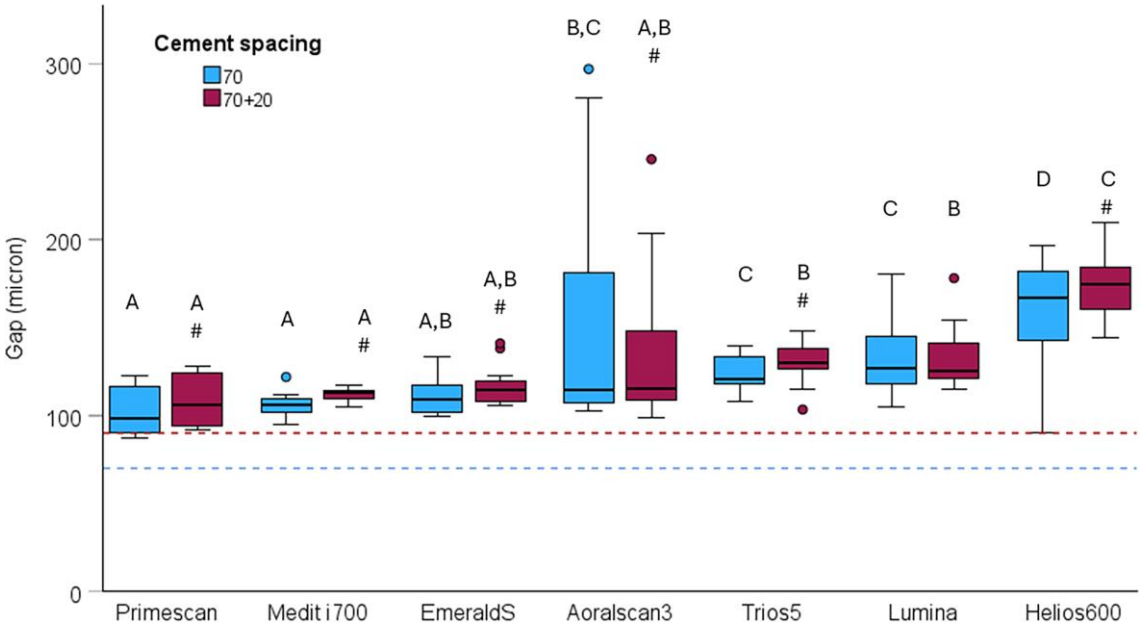


Figure 13. Comparison of the internal gap between IOSs and cement spacing groups. Different capital letters indicate a significant difference between IOSs within a cement spacing group at $p<0.05$, and # $p<0.05$ between cement spacing groups. The red and blue dotted line depicts the level of the two cement gap sets (24).

Table 7. Internal gaps (24).

	Cement spacing									
	70					70+20				
	N	Mean	Median	Q1	Q3	N	Mean	Median	Q1	Q3
Primescan	12	103	98	90	117	12	108	106	94	125
Medit i700	12	106	106	102	109	12	112	113	110	114
Emerald S	12	111	109	102	117	12	117	114	108	120
Aoralscan 3	12	155	114	108	181	12	137	115	109	148
Trios 5	12	124	120	118	133	12	130	130	126	138
Lumina	12	132	127	118	145	12	133	125	121	141
Helios 600	12	160	167	143	182	12	173	175	160	185

4.2.3 Mean absolute error (precision) of the marginal gap

The marginal gap was below the threshold value of 100 µm in Medit i700, Primescan, Emerald S, and Trios 5 in both cement spacing groups. The number of scans above the threshold was three in Lumina, four in Aoralscan 3, and eight in Helios 600 in group 70. After increasing the cement spacing (group 70+20), the number of scans above the

threshold decreased to two in Lumina and three in Aoralscan 3, but in Helios 600, it increased to ten (Figure 14).

The median MAE was significantly different between IOSs in both cement spacing groups. In group 70, the MAE in Medit i700, the Trios 5, and Emerald S were in the first-best homogenous subset, followed by Primescan. Lumina and Helios 600 were in the third subset, and Aoralscan 3 was in the fourth subset. The variabilities of Emerald S and Aoralscan 3 were decreased significantly by additional cement spacing (group 70+20). In group 70+20, the ranking was similar but with more overlaps between the subsets (Figure 15).

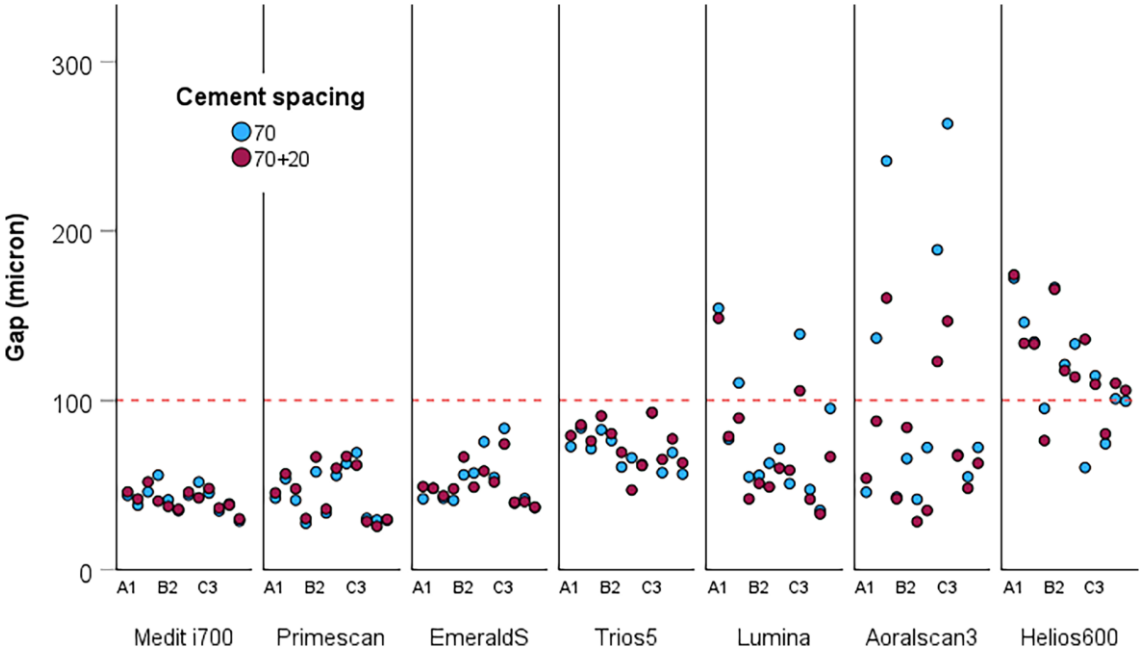


Figure 14. The marginal gap of designs made upon individual scans grouped by IOSs.

The blue dots indicate designs with 70 µm internal cement spacing, and the red dots indicate the designs created with 90 µm internal cement spacing and 20 µm cement spacing at the margin. The green dotted line depicts the 100 µm clinically acceptable limit (24).

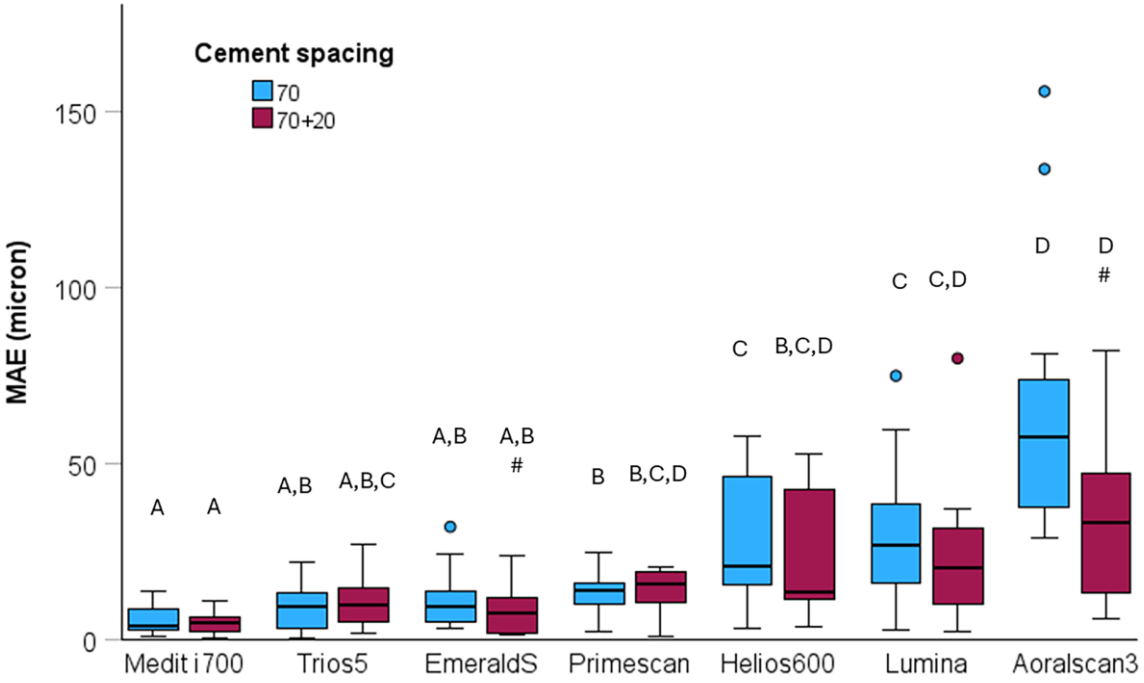


Figure 15. The variability of the marginal gap in different IOSs and cement spacing groups. Different capital letters indicate a significant difference between IOSs within a cement spacing group at $p<0.05$, and # indicates a significant difference between cement spacing groups at $p<0.05$ (24).

4.2.4 Mean absolute error (precision) of the internal gap

The median MAE was significantly different between IOSs in both cement spacing groups. In group 70, the MAE in Medit i700, the Trios 5, and Emerald S were in the first-best homogenous subset, followed by Primescan and Lumina. Helios 600 was in the third subset, and Aoralscan 3 was in the fourth subset. The variability of Aoralscan 3 decreased significantly by additional cement spacing (group 70+20). In group 70+20, the ranking was similar but with more overlaps between the subsets (Figure 16).

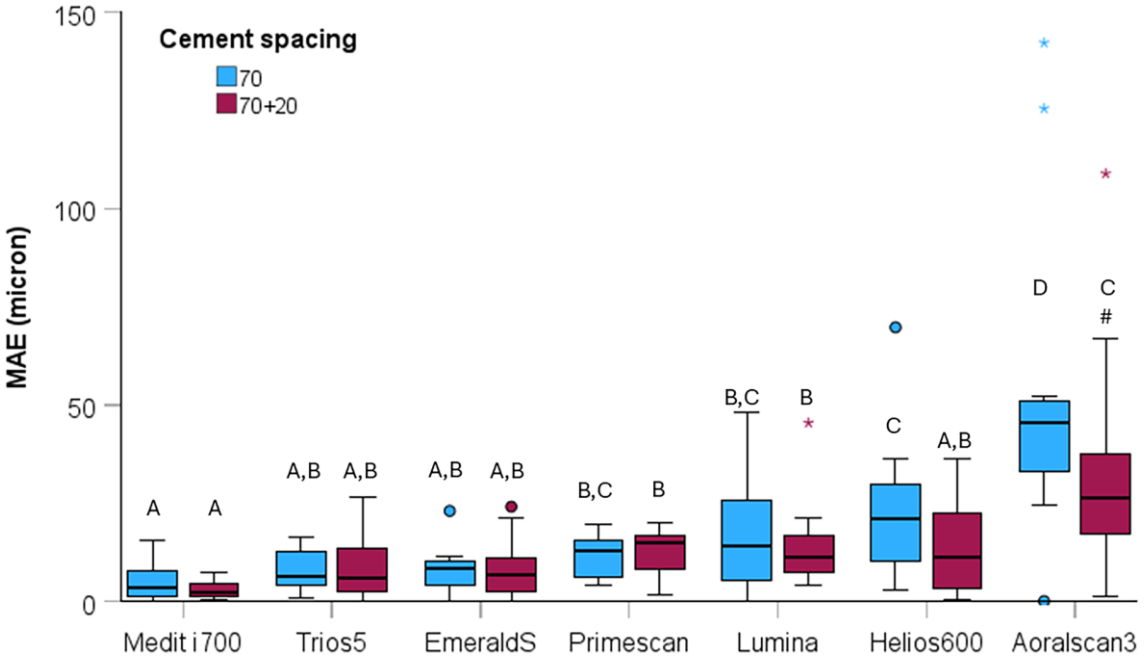


Figure 16. The variability of the internal gap in different IOSs and cement spacing groups. Different capital letters indicate a significant difference between IOSs within a cement spacing group at $p<0.05$, and # groups at $p<0.05$ between cement spacing groups (24).

5. DISCUSSION

The results of the thesis highlights that the accuracy of CAD/CAM workflow for fixed prosthetic restorations is strongly influenced by intraoral scanner performance, cement space settings, and the method used to evaluate restoration fit. Virtual-fit analysis using non-penetrating alignment provides a more realistic assessment of marginal and internal gaps than conventional trueness methods, which tend to underestimate discrepancies and might fail to detect clinically relevant outliers. Minor deviations from preset cement gap values were found to be clinically negligible and were mainly attributed to STL file resolution limitations rather than alignment errors, confirming the reliability of the virtual-fit approach for evaluating restoration adaptation.

Scanner performance also played a significant role in restoration accuracy. Newer-generation IOS systems from established manufacturers demonstrated superior trueness and precision, while older systems or less optimized scanners showed greater variability and occasional clinically unacceptable marginal gaps (46). These results indicate that both hardware and software improvements remain necessary to ensure predictable outcomes in complete-arch digital workflows (47). Notably, the study confirmed that scanners with similar conventional trueness values may exhibit markedly different clinical behavior when evaluated using non-penetrating alignment, underscoring the limitations of traditional accuracy metrics. Overall, the ideal cement spacing for CAD/CAM fixed restorations appears to lie between 70 and 90 μm, balancing restoration adaptation, marginal integrity, and long-term mechanical stability. Despite the limitations of *in vitro* design, both studies support the use of virtual-fit assessment as a more clinically relevant method for evaluating complete digital workflows in fixed prosthodontics.

5.1 Application of the virtual-fit method for fixed complete denture cases designed on intraoral scans: Effect of cement spacing – Study 1 *(in vitro)*

The first null hypothesis, which stated that the gaps calculated using the virtual-fit alignment method would not significantly differ from the predetermined cement gap values, was rejected. Nevertheless, in the absence of additional cement spacing (groups 70 and 140), the observed discrepancies were minimal, with errors below 4 μm internally and 13 μm at the marginal level, indicating negligible deviation from the intended cement gap values. A major contribution of this work lies in the validation of the virtual-fit alignment method, which restricts surface penetration during iterative closest point (ICP) alignment. Unlike conventional scan-to-scan trueness assessments, which allow unrealistic mesh interpenetration, the virtual-fit approach more closely simulates the physical seating of a restoration on prepared abutments. The measured deviation from the preset cement space was minimal (generally below 15 μm), confirming that the algorithm can reliably reproduce intended spacing and that any residual discrepancy is likely attributable to STL resolution limits rather than alignment errors. This is particularly relevant given that the magnitude of this deviation is well below clinically detectable thresholds and comparable to the resolution limits of established fit assessment techniques such as micro-CT (48), where the values range between 9 and 15 μm and optical coherence tomography (49) with a values of 12 μm axial and a 22 μm lateral resolution.

The second null hypothesis was partially rejected, as it proposed that the measured gap values would not differ significantly among the various cement gap settings. No significant differences were observed in the median internal error values between the spacing groups for any of the intraoral scanners evaluated. These findings suggest that a cement space setting of 70 μm may adequately compensate for inaccuracies associated with complete-arch intraoral scanning. Nevertheless, although median deviation values provide information regarding trueness, they do not reflect the distribution or variability of the data, which is indicative of precision. The effect of cement spacing on internal fit revealed that increasing internal spacing beyond 70 μm did not improve compensation for scanning inaccuracies. Median internal errors were not significantly different across spacing groups, indicating that a 70 μm cement gap is generally sufficient for complete-arch tooth-supported restorations. However, analysis of individual scans highlighted a

critical limitation of relying solely on median values: suboptimal IOS scans produced extreme internal and marginal discrepancies that were not adequately mitigated by standard spacing. In these cases, the addition of a modest 20 μm marginal and internal spacing (70+20 group) substantially reduced misfit, suggesting that limited additional spacing can act as a safeguard against imprecision rather than inaccuracy per se. Nevertheless, 70 μm is recommended as the minimum cement space to let the cement properly flow across internal gap and minimize the restoration elevation (50). Our findings support previous research on fabricated restorations, indicating that the optimal cement spacing is approximately 70 μm, with a slight additional space recommended for extended scan areas where intraoral scanner accuracy tends to decrease (51). In contrast, excessive cement spacing (140 μm) proved counterproductive, particularly at the margin. Although larger gaps might intuitively appear beneficial for accommodating scan errors, the results demonstrated increased marginal discrepancies in case of total internal gaps approached by 170–190 μm. Such values exceed ranges previously associated with optimal retention and may compromise bonding effectiveness or increase the risk of debonding and mechanical failure. These findings align with prior biomechanical and experimental studies indicating that excessive cement thickness negatively influences stress distribution and retention strength (52). Consequently, indiscriminate enlargement of cement space cannot be recommended as a strategy to offset scanning inaccuracies (53).

AI-based cement space setting in CAD/CAM restorations has the potential to significantly improve the accuracy and clinical fit of indirect restorations (11, 54). Cement gap parameters are typically standardized and manually adjusted by the operator. However, these settings may not adequately compensate for variations in preparation geometry, milling limitations, or material-specific behavior (16). AI-driven systems can analyze large datasets derived from intraoral scans, preparation designs, milling performance, and clinical outcomes to automatically optimize cement space distribution for each individual restoration (55). By dynamically adapting the cement gap according to tooth morphology, restoration material, and manufacturing constraints, AI-assisted CAD software may enhance marginal adaptation and internal fit while reducing seating discrepancies and excessive cement thickness (56).

The third null hypothesis, which proposed the absence of a significant correlation between the virtual-fit approach and the conventional trueness assessment method, was rejected. Both methods yielded comparable outcomes regarding the comparison of intraoral scanners and demonstrated a significant positive correlation. These findings support the validity of previous studies that used conventional trueness measurements for comparative evaluation of IOS systems. However, the present results indicated that the conventional method substantially underestimates the actual trueness of intraoral scanners. Furthermore, this approach failed to identify outliers, suggesting limited sensitivity to scan-to-scan variability and imprecision. Consequently, the conventional trueness method may not accurately predict the clinical misfit of restorations. Therefore, the acceptable accuracy of intraoral scanners for complete-arch restorations cannot be reliably determined solely on the basis of conventional trueness measurements. This highlights a fundamental limitation of conventional trueness evaluations: although they may suffice for relative comparison between scanners, they do not provide a reliable basis for predicting restoration fit or clinical acceptability in complete-arch prosthodontics.
Several limitations should be acknowledged. The *in vitro* design, reliance on rigid 3D-printed models, and absence of clinical variables such as saliva, patient movement with soft-tissue dynamics, and periodontal ligament compliance may limit direct extrapolation to *in vivo* conditions (57). Furthermore, fabrication-related errors were intentionally excluded, and future studies should integrate manufacturing and clinical try-in data to fully validate the predictive value of the virtual-fit method (58). Nevertheless, the use of stable 3D-printed models, experienced operators, and up-to-date software versions strengthens the internal validity of the findings.

5.2 Complete-arch accuracy of seven intraoral scanners measured by the virtual-fit method – Study 2 *(in vitro)*

The fourth null hypothesis was partially rejected because the mean marginal and internal gap values, representing trueness, were comparable for the Medit i700, Primescan, and Emerald S scanners and were lower than those observed for the other intraoral scanners evaluated. In terms of precision, reflected by the variability of the gap measurements, the Medit i700, Trios 5, and Emerald S scanners demonstrated similar performance and exhibited lower variation compared with the remaining IOS systems.

The fifth null hypothesis was likewise partially rejected, as an increase in cement space setting significantly reduced the marginal and internal gap values in certain scanners that initially demonstrated lower trueness.

The study expanded the application of the virtual-fit method by comparing the complete-arch accuracy of seven contemporary intraoral scanners, thereby providing clinically relevant insight into scanner performance under conditions that closely simulate the fabrication of fixed complete-arch restorations. Unlike conventional scan-to-scan accuracy assessments, which tend to underestimate clinically meaningful discrepancies due to penetrating alignment algorithms, the virtual-fit method employed in this study offers a more realistic prediction of marginal and internal fit by preventing virtual penetration of the restoration design into the reference model (26).

The findings demonstrated that Emerald S, Medit i700, Primescan, and Trios 5 achieved marginal and internal gaps well within clinically acceptable limits for tooth-borne complete-arch restorations. These results corroborate earlier evidence suggesting that established IOS manufacturers, particularly when using the latest software versions, can produce scans suitable for extended fixed prostheses (59). The favorable performance of these scanners highlights the impact of continuous software and hardware refinement, which appears to mitigate cumulative stitching errors that have historically limited full-arch digital impressions (60).

In the case of Medit i700 using a slighlty different software version (2.4.4), similarly lower trueness values were reported compared to the present study, measuring 42 µm for the mandibular arch and 54 µm for the maxillary arch in a human cadaver with natural dentition (61). A newer software version (2.5.7) resulted in a better trueness value of 24 µm on a plastic model (62). Overall, the improved results observed in this study were likely attributable to the operator's experience, the use of a homogeneous plastic substrate, and the implementation of the latest software version (3.1.4) compared with previous investigations (47). Previous studies reported Primescan trueness values ranging from 19–26 µm in dental and plastic models using older software versions (5.1–5.1.3), while values increased to 40–51 µm in human cadavers and partially edentulous models (63). In the present study, the latest software version (5.2.4) provided excellent marginal gap results, highlighting the positive effect of software updates on scanning accuracy (26). Regarding to Emerald S with a slightly older version of Romexis software (6.2.1)

and with an experienced user, the trueness resulted in a mean value of 20 μm (47). Despite findings, trueness remained lower than in the present study, partly due to methodological differences between penetrating and non-penetrating alignment. With a newer software version (6.3.2), trueness values of 33 μm and 50 μm were reported for the mandibular and maxillary arches, although measurements were performed on a human cadaver with natural teeth (61). Similarly, a recent virtual-fit study reported slightly lower trueness values (64–66 μm) than the present results (45–48 μm), which may be explained by the use of an inexperienced operator and an older software version (6.0.1) (47). As observed with Medit i700, improved outcomes were likely associated with operator experience and the latest software version (6.4.5) (64).

In contrast, Lumina, Aoralscan 3 and Trios 5 exhibited greater variability in marginal accuracy despite mean values remaining below the 100 μm threshold. This inconsistency suggests that while these scanners are able to generate accurate complete-arch scans, their precision may be more sensitive to operator experience, scanning strategy, or software maturity. Notably, the relatively recent release of iTero Lumina, which is primarily optimized for orthodontic workflows, is likely to influence its performance in a restorative environment. Nevertheless, the significant reduction in marginal gaps observed after increasing cement spacing indicates that suboptimal scan accuracy can be partially compensated during the CAD phase, reinforcing the clinical importance of individualized cement space settings (59). Recent studies indicate that the Aoralscan 3 intraoral scanner provides clinically acceptable accuracy for complete-arch digital impressions and may be suitable for extended fixed prosthodontic workflows, although precision improvements are still desirable for some scans (65). Previous Aoralscan model from the Shining manufacturer in a complete-arch dentition model showed comparable linear measurement accuracy to Trios 3, Trios 4, iTero Element 2, iTero Element 5D, Dental Wings, Panda, Medit i500, and Emerald S (66). Since Trios 5 was introduced in 2023, available data remains limited. Existing studies have assessed trueness either in single crown preparations (63), complete-arch linear measurements (67), or using reverse optical impressions in edentulous implant cases (68), which limits direct comparison with the present results (66). For single crown margins, Trios 5 (17.3 software version 1.1), Primescan (software version not specified), and Medit i700 (3.0.3) showed comparable trueness and precision, which contrasts with the findings of the current study. Similarly,

in reverse optical implant impressions, Trios 5 demonstrated performance comparable to Medit i700 and superior to Primescan in terms of both trueness and precision (68).

Helios 600 demonstrated inferior trueness and precision compared with the other scanners evaluated, consistently exceeding recommended marginal limits. This finding suggests that not all IOS systems currently available on the market are suitable for complete-arch fixed restorations when evaluated using clinically realistic alignment criteria. These results emphasize the necessity of application-specific validation of IOS technology rather than extrapolating performance from single-unit or short-span studies. Recent studies indicate that the Helios 600 intraoral scanner demonstrates moderate precision but lower trueness in complete-arch fixed prosthodontic workflows compared with more established systems such as Primescan, Medit i700, and Trios 5, particularly regarding marginal gap adaptation (69).

A key contribution of this study lies in confirming the beneficial effect of increasing cement space setting on restoration fit, specifically a configuration of 70 µm internal spacing with an additional 20 µm at the margin. This aligns with the theoretical framework that cement spacing can compensate for scanning inaccuracies and supports the concept that acceptable marginal adaptation should be assessed as part of an integrated digital workflow rather than as an isolated scanning outcome (70).

Internal and marginal gap changes showed a parallel trend, with similar IOS rankings observed for both parameters. Analysis of these findings indicates that the optimal cement spacing lies between 70 and 90 µm, in agreement with recent literature on the relationship between cement space and fit in CAD/CAM restorations (71). Accordingly, further improvements in IOS hardware and software are required to reduce inaccuracies and ensure that a cement space of up to 90 µm is sufficient to compensate for existing scanning errors.

Several limitations should be acknowledged. This study did not evaluate internal cement gap settings exceeding 90 µm (70 + 20 µm). Therefore, it remains unclear whether larger spacer values could compensate for inaccurate scans. Previous research has shown that adding 20 µm of cement space may reduce marginal discrepancies in suboptimal scans; however, a 140 µm cement setting did not yield a statistically significant improvement (26). Consequently, spacer values above 90 µm were not included in the present investigation. The *in vitro* design excluded clinical variables such as patient-releted

circumstances (saliva etc.) which may further affect scan accuracy *in vivo* (72). Another potential source of bias is that all scans were performed by an experienced operator. In contrast, newer intraoral scanners are often used by less experienced clinicians in routine practice. The iTero Lumina was released in 2024, the Helios 600 within the past four years, and the Aoralscan 3 has been available in Europe for five years. Therefore, the comparatively lower performance observed for these systems may be partly attributed to limited user experience and reduced iterative feedback to manufacturers. Additionally, although experienced operators were used to reduce variability, real-world clinical settings may introduce a broader range of operator proficiency. Future research should therefore validate the virtual-fit method under clinical conditions and explore its predictive value by correlating virtual measurements with the fit of manufactured restorations.

In summary, this study reinforces the virtual-fit method as a robust and clinically meaningful approach for evaluating IOS accuracy in complete-arch restorations. The results provide practical guidance for scanner selection and CAD parameter optimization, supporting the expanding role of intraoral scanning in full-arch digital prosthodontics.

6. CONCLUSIONS

6.1 Application of the virtual-fit method for fixed complete denture cases designed on intraoral scans: Effect of cement spacing – Study 1

1. Validation of the virtual-fit alignment algorithm

The virtual-fit method reliably simulates the intended cement space configuration while preventing surface interpenetration during ICP alignment.

Measured internal and marginal gaps corresponded closely to the predefined cement space settings, confirming that the virtual-fit method realistically emulates the clinical seating behavior of tooth-supported fixed dental prostheses.

Null hypothesis #1 was rejected.

2. Effect of cement spacing on restoration fit and scanner accuracy

Cement spacing significantly affected internal and marginal adaptation.

A baseline internal cement space of 70 µm without marginal spacing was adequate for most complete-arch restorations produced from high-performing IOS systems such as Emerald S and Medit i700. The addition of 20 µm marginal cement space improved seating and compensated for misfit in suboptimal scans, whereas excessive cement spacing (140 µm) negatively affected adaptation. Therefore, a cement gap setting of 70 + 20 µm is suggested.

Null hypothesis #2 was partly rejected.

3. Relationship between the virtual-fit method and conventional trueness measurements

The virtual-fit method identified clinically relevant discrepancies and suboptimal scans that remained undetected by conventional scan-to-scan trueness analyses.

These findings indicate that conventional trueness measurements may underestimate clinically relevant prosthetic misfit because of artificial deviation minimization caused by interpenetrating alignment algorithms. The observed relationship between the two approaches showed that conventional trueness values alone do not fully reflect clinically meaningful restoration fit.

Null hypothesis #3 was rejected.

6.2 Complete-arch accuracy of seven intraoral scanners measured by the virtual-fit method – Study 2

1. Comparison of complete-arch accuracy among seven intraoral scanners

The findings demonstrated statistically significant differences among scanners.

Medit i700, Primescan, Emerald S, and Trios 5 consistently produced internal and marginal fit values meeting clinical requirements for tooth-supported complete-arch restorations.

Lumina and Aoralscan 3 demonstrated clinically acceptable performance but showed greater variability, suggesting higher sensitivity to scanning strategy and operator experience.

In contrast, Helios 600 failed to meet clinical accuracy requirements under clinically realistic alignment conditions.

Null hypothesis #4 was rejected.

2. Effect of two cement spacings across intraoral scanner accuracy

Cement spacing significantly influenced restoration fit across scanners.

A configuration consisting of 70 µm internal cement space combined with an additional 20 µm marginal space (90 [70+20] µm total configuration) consistently optimized restoration seating by compensating for scanning inaccuracies while preserving internal and marginal adaptation. Therefore, a cement gap setting of 70 + 20 µm is suggested.

Null hypothesis #5 was rejected.

7. SUMMARY

Objectives: The thesis aimed to introduce a clinically realistic method for evaluating IOS accuracy in tooth-supported complete-arch fixed prosthodontics fabricated by CAD/CAM system. The thesis also aimed to validate the virtual-fit alignment method, to assess the influence of cement spacing on compensating scanning inaccuracies, and to compare the complete-arch accuracy of different IOSs using clinically interpretable fit parameters.

Methods: In the first study, four maxillary models were scanned using an industrial reference scanner, Emerald S, and Medit i700 IOSs. Complete-arch fixed frameworks were designed with three different cement space settings: 70 µm, 70+20 µm, and 140 µm. Frameworks were aligned to the reference scan using virtual-fit alignment simulating clinical seating. Internal and marginal gaps were measured and correlated with conventional trueness values. In the second study, also four maxillary models were scanned using seven IOSs (Aoralscan 3, Emerald S, Helios 600, Lumina, Medit i700, Primescan, and Trios 5). Digital frameworks were designed with 70 and 70+20 µm spacing. Internal and marginal gaps were evaluated using the validated virtual-fit method.

Results: The virtual-fit method accurately reproduced preset cement spacing with deviations of 3–13 µm. Conventional trueness metrics correlated with virtual-fit measurements but underestimated clinically relevant misfit by 2.6–4.6 times and failed to detect extreme discrepancies. A baseline internal cement space of 70 µm was sufficient for most scans, while an additional 20 µm marginal spacing improved fit in suboptimal scans; excessive spacing (140 µm) adversely affected marginal adaptation. Emerald S, Medit i700, Primescan, and Trios 5 met fit requirements for complete-arch restorations, whereas Lumina and Aoralscan3 showed greater variability and Helios 600 did not meet accuracy criteria. Increased cement spacing improved fit for less precise scanners.

Conclusions: The virtual-fit method enables clinically meaningful evaluation of IOS accuracy in complete-arch fixed prosthodontics produced by CAD/CAM system. Cement spacing is a critical, workflow-dependent parameter, and conventional trueness metrics alone are insufficient to predict restoration fit. The findings support evidence-based scanner selection and CAD design optimization for reliable full-arch digital workflows.

8. REFERENCES

1. Abduo J, Lyons K, Swain M. Fit of zirconia fixed partial denture: a systematic review. J Oral Rehabil. 2010;37(11):866-76.
2. Contrepois M, Soenen A, Bartala M, Laviole O. Marginal adaptation of ceramic crowns: a systematic review. J Prosthet Dent. 2013;110(6):447-54.e10.
3. Romandini P, Pjetursson BE, Pitta J, Balet A, Ikumi R, Sailer I. A Systematic Review and Meta-Analysis Evaluating the Survival, the Failure and the Complication Rates of Metal-Ceramic, Veneered and Monolithic All-Ceramic Tooth-Supported Multiple- Unit Fixed Dental Prostheses (Fdps). Int J Prosthodont. 2026;0(0):1-34.
4. Hewlett ER, Atchison KA, White SC, Flack V. Radiographic secondary caries prevalence in teeth with clinically defective restorations. J Dent Res. 1993;72(12):1604-8.
5. Lang NP, Kiel RA, Anderhalden K. Clinical and microbiological effects of subgingival restorations with overhanging or clinically perfect margins. J Clin Periodontol. 1983;10(6):563-78.
6. Heintze SD. Clinical relevance of tests on bond strength, microleakage and marginal adaptation. Dent Mater. 2013;29(1):59-84.
7. Sasany R, Yilmaz B. Marginal discrepancy and fracture load of thermomechanically fatigued crowns fabricated with different CAD-CAM techniques. J Prosthodont. 2023;32(7):602-7.
8. McLean JW, von F. The estimation of cement film thickness by an in vivo technique. British dental journal. 1971;131(3):107-11.
9. Holmes JR, Bayne SC, Holland GA, Sulik WD. Considerations in measurement of marginal fit. J Prosthet Dent. 1989;62(4):405-8.
10. Saravi B, Vollmer A, Hartmann M, Lang G, Kohal RJ, Boeker M, Patzelt SBM. Clinical Performance of CAD/CAM All-Ceramic Tooth-Supported Fixed Dental Prostheses: A Systematic Review and Meta-Analysis. Materials (Basel). 2021;14(10).
11. Schwendicke F, Samek W, Krois J. Artificial Intelligence in Dentistry: Chances and Challenges. J Dent Res. 2020;99(7):769-74.
12. Mangano F, Gandolfi A, Luongo G, Logozzo S. Intraoral scanners in dentistry: a review of the current literature. BMC Oral Health. 2017;17(1):149.

13. Vág J, Nagy Z, Simon B, Mikolicz Á, Kövér E, Mennito A, et al. A novel method for complex three-dimensional evaluation of intraoral scanner accuracy. Int J Comput Dent. 2019;22(3):239-49.
14. Nagy Z, Simon B, Mennito A, Evans Z, Renne W, Vág J. Comparing the trueness of seven intraoral scanners and a physical impression on dentate human maxilla by a novel method. BMC Oral Health. 2020;20(1):97.
15. Ho SP, Kurylo MP, Fong TK, Lee SS, Wagner HD, Ryder MI, Marshall GW. The biomechanical characteristics of the bone-periodontal ligament-cementum complex. Biomaterials. 2010;31(25):6635-46.
16. Khanagar SB, Al-Ehaideb A, Maganur PC, Vishwanathaiah S, Patil S, Baeshen HA, et al. Developments, application, and performance of artificial intelligence in dentistry - A systematic review. J Dent Sci. 2021;16(1):508-22.
17. Vitai V, Németh A, Sólyom E, Czumbel LM, Szabó B, Fazekas R, et al. Evaluation of the accuracy of intraoral scanners for complete-arch scanning: A systematic review and network meta-analysis. J Dent. 2023;137:104636.
18. Jemt T, Hjalmarsson L. In Vitro Measurements of Precision of Fit of Implant-Supported Frameworks. A Comparison between "Virtual" and "Physical" Assessments of Fit Using Two Different Techniques of Measurements. Clinical Implant Dentistry and Related Research. 2012;14(s1):e175-e82.
19. Rhee YK, Huh YH, Cho LR, Park CJ. Comparison of intraoral scanning and conventional impression techniques using 3-dimensional superimposition. J Adv Prosthodont. 2015;7(6):460-7.
20. Buhl J, Mehl A, Ender A. An in-vitro study on factors influencing the accuracy of current intraoral scanners. Sci Rep. 2025;15(1):41049.
21. DeFee M, Renne W, Shazib MA, Queiroz A, Mennito A, Borbola D, Vag J. Virtual-Fit Assessment of Full-Arch Implant Photogrammetry Accuracy in a Human Cadaver Model. J Dent. 2026:106668.
22. Kim RJ, Park JM, Shim JS. Accuracy of 9 intraoral scanners for complete-arch image acquisition: A qualitative and quantitative evaluation. J Prosthet Dent. 2018;120(6):895-903.e1.

23. Borbola D, Vag J. Unifying intraoral scanner, computer-aided manufacturing, and final crown accuracy: A virtual-fit method for marginal gap evaluation. J Dent. 2025;163:106113.
24. Borbola D, Mikolicz A, Romanszky L, Sersli G, DeFee M, Renne W, Vag J. Complete-arch accuracy of seven intraoral scanners measured by the virtual-fit method. J Dent. 2024;149:105281.
25. Kim D, Jeon MJ, Kang YS, Choi YS, Park JK, Seo DG. Effect of axiopulpal line angle design and cement space settings on seating accuracy of CAD/CAM ceramic inlays: an in vitro study. J Dent. 2026:106677.
26. Vag J, Romanszky L, Sersli G, DeFee M, Renne W, Mangano F, Borbola D. Application of the virtual-fit method for fixed complete denture cases designed on intraoral scans: Effect of cement spacing. J Dent. 2024;141:104780.
27. Loetzerich JM, Raith S, Reich S. Verification of a digital approach for three-dimensional evaluation of marginal and internal fit. J Prosthet Dent. 2025;134(1):160-6.
28. Sorensen JA. A standardized method for determination of crown margin fidelity. J Prosthet Dent. 1990;64(1):18-24.
29. Molin M, Karlsson S. The fit of gold inlays and three ceramic inlay systems. A clinical and in vitro study. Acta Odontol Scand. 1993;51(4):201-6.
30. Hupe VM, Beuer F, Sterzenbach G, Adali U. Comparison of marginal and internal fit of 10-unit fixed dental prostheses fabricated from cobalt chromium alloys or zirconia ceramics using digital workflows. J Prosthet Dent. 2025;134(3):761.e1-.e8.
31. Nawafleh NA, Mack F, Evans J, Mackay J, Hatamleh MM. Accuracy and reliability of methods to measure marginal adaptation of crowns and FDPs: a literature review. J Prosthodont. 2013;22(5):419-28.
32. Groten M, Axmann D, Pröbster L, Weber H. Determination of the minimum number of marginal gap measurements required for practical in-vitro testing. J Prosthet Dent. 2000;83(1):40-9.
33. Holst S, Karl M, Wichmann M, Matta RE. A new triple-scan protocol for 3D fit assessment of dental restorations. Quintessence Int. 2011;42(8):651-7.
34. Bernauer SA, Zitzmann NU, Joda T. The Complete Digital Workflow in Fixed Prosthodontics Updated: A Systematic Review. Healthcare (Basel). 2023;11(5).

35. GmbH G. 2019 [Available from: https://scanare3d.com/wp-content/uploads/2020/07/GOM_Brochure_Redesign_ATOS-Capsule_EN.pdf.
36. report Dp. 2019 [Available from: https://www.dentalproductsreport.com/view/planmeca-launches-emeraldtm-s-intraoral-scanner.
37. dentistry Iod. 2021 [Available from: https://instituteofdigitaldentistry.com/cad-cam/medit/medit-i700-review/.
38. [Available from: https://www.shining3ddental.com/solution/aoralscan-3/.
39. Align Technology [Available from: https://investor.aligntech.com/news-releases/news-release-details/align-technology-announces-new-itero-luminatm-intraoral-scanner/.
40. Eighteeth [Available from: https://www.eighteeth.com/Intraoral-Scanner/71.html.
41. Dentsply Sirona US [Available from: https://www.dentsplysirona.com/en-us/discover/discover-by-brand/primescan.html.
42. 3Shape [Available from: https://www.3shape.com/en/blog/2023/tips-perfect-trios-scan.
43. Faul F, Erdfelder E, Lang AG, Buchner A. G*Power 3: a flexible statistical power analysis program for the social, behavioral, and biomedical sciences. Behav Res Methods. 2007;39(2):175-91.
44. Cohen J. Statistical Power Analysis for the Behavioral Sciences (2nd ed.): Routledge.; 1988.
45. Chai T, Draxler RR. Root mean square error (RMSE) or mean absolute error (MAE)? – Arguments against avoiding RMSE in the literature. Geosci Model Dev. 2014;7(3):1247-50.
46. Sanda M, Miyoshi K, Baba K. Trueness and precision of digital implant impressions by intraoral scanners: a literature review. Int J Implant Dent. 2021;7(1):97.
47. Vág J, Renne W, Revell G, Ludlow M, Mennito A, Teich ST, Gutmacher Z. The effect of software updates on the trueness and precision of intraoral scanners. Quintessence Int. 2021;52(7):636-44.

48. Tabata LF, de Lima Silva TA, de Paula Silveira AC, Ribeiro APD. Marginal and internal fit of CAD-CAM composite resin and ceramic crowns before and after internal adjustment. J Prosthet Dent. 2020;123(3):500-5.
49. Al-Imam H, Michou S, Benetti AR, Gotfredsen K. Evaluation of marginal and internal fit of acrylic bridges using optical coherence tomography. J Oral Rehabil. 2019;46(3):274-81.
50. Grajower R, Zuberi Y, Lewinstein I. Improving the fit of crowns with die spacers. J Prosthet Dent. 1989;61(5):555-63.
51. Yehia A, Abo El Fadl A, El Sergany O, Ebeid K. Effect of different span lengths with different total occlusal convergences on the accuracy of intraoral scanners. J Prosthodont. 2024;33(3):252-8.
52. Son YH, Han CH, Kim S. Influence of internal-gap width and cement type on the retentive force of zirconia copings in pullout testing. J Dent. 2012;40(10):866-72.
53. Ha SR. Biomechanical three-dimensional finite element analysis of monolithic zirconia crown with different cement type. J Adv Prosthodont. 2015;7(6):475-83.
54. Yeslam HE, Freifrau von Maltzahn N, Nassar HM. Revolutionizing CAD/CAM-based restorative dental processes and materials with artificial intelligence: a concise narrative review. PeerJ. 2024;12:e17793.
55. Alfaifi MA. A Systematic Review of the Accuracy of Crowns Designed Using Artificial Intelligence Versus CAD/CAM and Traditional Methods. Medicina (Kaunas). 2026;62(3).
56. Papadiochou S, Pissiotis AL. Marginal adaptation and CAD-CAM technology: A systematic review of restorative material and fabrication techniques. J Prosthet Dent. 2018;119(4):545-51.
57. Agustín-Panadero R, Moreno DM, Pérez-Barquero JA, Fernández-Estevan L, Gómez-Polo M, Revilla-León M. Influence of type of restorative materials and surface wetness conditions on intraoral scanning accuracy. J Dent. 2023;134:104521.
58. Revell G, Simon B, Mennito A, Evans ZP, Renne W, Ludlow M, Vág J. Evaluation of complete-arch implant scanning with 5 different intraoral scanners in terms of trueness and operator experience. J Prosthet Dent. 2022;128(4):632-8.

59. Guimarães AS, Mendonça TS, Borella PS, Khalil G, Li J, Al-Tarawneh S, et al. Accuracy of intraoral scanners for full-arch implant scanning in the Maxilla using horizontal scanbody. PLoS One. 2025;20(12):e0332174.
60. Waldecker M, Rues S, Behnisch R, Rammelsberg P, Bömicke W. Effect of scan-path length on the scanning accuracy of completely dentate and partially edentulous maxillae. J Prosthet Dent. 2024;131(1):146-54.
61. Vag J, Stevens CD, Badahman MH, Ludlow M, Sharp M, Brenes C, et al. Trueness and precision of complete arch dentate digital models produced by intraoral and desktop scanners: An ex-vivo study. J Dent. 2023;139:104764.
62. Giuliodori G, Rappelli G, Aquilanti L. Intraoral Scans of Full Dental Arches: An In Vitro Measurement Study of the Accuracy of Different Intraoral Scanners. Int J Environ Res Public Health. 2023;20(6).
63. Revilla-León M, Gómez-Polo M, Barmak AB, Yilmaz B, Kois JC, Alonso Pérez-Barquero J. Influence of scan extension and starting quadrant on the accuracy of four intraoral scanners for fabricating tooth-supported crowns. J Prosthet Dent. 2025;134(4):1260-70.
64. Falih MY, Majeed MA. Trueness and Precision of Eight Intraoral Scanners with Different Finishing Line Designs: A Comparative In Vitro Study. Eur J Dent. 2023;17(4):1056-64.
65. Mikolicz Á, Simon B, Lőrincz G, Vág J. Clinical precision of Aoralscan 3 and Emerald S on the palatal and dentition areas: Evaluation for forensic applications. J Dent. 2025;153:105455.
66. Amornvit P, Rokaya D, Sanohkan S. Comparison of Accuracy of Current Ten Intraoral Scanners. Biomed Res Int. 2021;2021:2673040.
67. Schmalzl J, Keskeny G, Hermann P, Pál A, Géczi Z, Borbély J, Róth I. Evaluating the influence of palate scanning on the accuracy of complete-arch digital impressions-An in vitro study. J Dent. 2024;145:105014.
68. Nuytens P, Vandeweghe S, D'Haese R. Accuracy of a chairside reverse scanbody workflow for a complete arch implant-supported prosthesis using four intraoral scanners versus a desktop scanner. J Dent. 2023;138:104717.
69. Bedi A, Monisha J, Madhan B. Clarification regarding data interpretation in "Impact of dental crowding on the trueness and precision of intraoral scanners:

Comparison across different devices and techniques". Am J Orthod Dentofacial Orthop. 2026;169(3):263.
70. Goujat A, Abouelleil H, Colon P, Jeannin C, Pradelle N, Seux D, Grosgogeat B. Marginal and internal fit of CAD-CAM inlay/onlay restorations: A systematic review of in vitro studies. J Prosthet Dent. 2019;121(4):590-7.e3.
71. Pilecco RO, Machry RV, Baldi A, Tribst JPM, Sarkis-Onofre R, Valandro LF, et al. Influence of CAD-CAM milling strategies on the outcome of indirect restorations: A scoping review. J Prosthet Dent. 2024;131(5):811.e1-.e10.
72. Alkadi L. A Comprehensive Review of Factors That Influence the Accuracy of Intraoral Scanners. Diagnostics (Basel). 2023;13(21).

9. BIBLIOGRAPHY OF PUBLICATIONS

9.1 Publications directly related to the thesis:

- **Borbola D**, Mikolicz A, Romanszky L, Sersli G, DeFee M, Renne W, Vag J. *Complete-arch accuracy of seven intraoral scanners measured by the virtual-fit method.* Journal of Dentistry, 2024 Oct;149:105281. https://doi.org/10.1016/j.jdent.2024.105281
  Impact factor: 5,5 (ranking: D1)

- Vag J, Romanszky L, Sersli G, DeFee M, Renne W, Mangano F, **Borbola D**. *Application of the virtual-fit method for fixed complete denture cases designed on intraoral scans: Effect of cement spacing*. Journal of Dentistry, 2024 Feb;141:104780. https://doi.org/10.1016/j.jdent.2023.104780
  Impact factor: 5,5 (ranking: D1)

9.2 Publications indirectly related to the thesis:

- DeFee M, Renne W, Shazib MA, Queiroz A, Mennito A, **Borbola D**, Vag J. *Virtual-fit assessment of full-arch implant photogrammetry accuracy in a human cadaver model.* Journal of Dentistry, 2026 Jul;170:106668. https://doi.org/10.1016/j.jdent.2026.106668
  Impact factor: 5,8 (ranking: D1),

- **Borbola D**, Vag J. *Unifying intraoral scanner, computer-aided manufacturing, and final crown accuracy: A virtual-fit method for marginal gap evaluation.* Journal of Dentistry, 2025 Dec;163:106113. https://doi.org/10.1016/j.jdent.2025.106113
  Impact factor: 5,8 (ranking: D1)

- **Borbola D**, Berkei G, Simon B, Romanszky L, Sersli G, DeFee M, Renne W, Mangano F, Vag J. *In vitro comparison of five desktop scanners and an industrial scanner in the evaluation of an intraoral scanner accuracy*. Journal of Dentistry, 2023 Feb;129:104391. https://doi.org/10.1016/j.jdent.2022.104391
  Impact factor: 4,8 (ranking: D1)

Cumulative impact factor: 27,4

10. ACKNOWLEDGEMENTS

I would like to express my sincere gratitude to Professor János Vág, my mentor and supervisor, for his invaluable guidance, support, and trust throughout my doctoral studies. His expertise, constructive advice, and encouragement have been essential to the completion of this dissertation. I am particularly grateful for his assistance with the statistical analyses and for the confidence he placed in me throughout this journey.

I would like to extend my heartfelt thanks to Dr. Beáta Kerémi for her outstanding support in the formal finalization and preparation of the dissertation. I am also sincerely grateful to Dr. Eszter Szalai for undertaking the internal review of the dissertation. Their guidance, support, and assistance during the final stages of the dissertation were invaluable, and I greatly appreciate their contributions to its final refinement.

I am also deeply grateful to my family, especially to Kata and to my parents, who accompanied and supported me throughout my journey as a doctoral student. Their unwavering encouragement, patience, and understanding meant a great deal to me, particularly during the many weekends devoted to research and writing. Their constant support helped me persevere and successfully complete this dissertation.

I am also grateful for the opportunity to have served the university community for several years as a member of the Doctoral Students' Association Board and later as its Vice President. This experience added a valuable and enriching dimension to my doctoral years and allowed me to represent and advocate for fellow doctoral students with a strong sense of responsibility and commitment.

I would also like to express my sincere appreciation to the members of the evaluation committee for their time, effort, and valuable comments on this dissertation. Their insightful feedback and constructive suggestions have greatly contributed to the improvement of this work.

Last but not least, I would like to thank all my colleagues at the Department of Restorative Dentistry and Endodontics for their support, encouragement, and assistance throughout my doctoral studies.